

**DOT/FAA/AR-07/42,P3**

Federal Aviation Administration  
William J. Hughes Technical Center  
Aviation Research Division  
Atlantic City International Airport  
New Jersey 08405

# **Design and Quality Assurance Premium Quality Aerospace Castings**

## **Part 3: Static Strength Assessment of Boeing 757 EE Access Door**

March 2020

Final Report

This document is available to the U.S. public through the National Technical Information Services (NTIS), Springfield, Virginia 22161.

This document is also available from the Federal Aviation Administration William J. Hughes Technical Center at [actlibrary.tc.faa.gov](http://actlibrary.tc.faa.gov).



U.S. Department of Transportation  
**Federal Aviation Administration**

## **NOTICE**

This document is disseminated under the sponsorship of the U.S. Department of Transportation in the interest of information exchange. The U.S. Government assumes no liability for the contents or use thereof. The U.S. Government does not endorse products or manufacturers. Trade or manufacturers' names appear herein solely because they are considered essential to the objective of this report. The findings and conclusions in this report are those of the author(s) and do not necessarily represent the views of the funding agency. This document does not constitute FAA policy. Consult the FAA sponsoring organization listed on the Technical Documentation page as to its use.

This report is available at the Federal Aviation Administration William J. Hughes Technical Center's Full-Text Technical Reports page: [actlibrary.tc.faa.gov](http://actlibrary.tc.faa.gov) in Adobe Acrobat portable document format (PDF).

# Technical Report Documentation Page

1. Report No. DOT/FAA/AR-07/42,P3		2. Government Accession No.		3. Recipient's Catalog No.	
4. Title and Subtitle STATIC STRENGTH ASSURANCE PREMIUM QUALITY AEROSPACE CASTINGS, PART 3: STATIC STRENGTH ASSESSMENT OF BOEING 757 EE ACCESS DOOR				5. Report Date March 2020	
				6. Performing Organization Code ANG-E28	
7. Author(s) Brian Moran, Stephane Bordas, and James G. Conley				8. Performing Organization Report No.	
9. Performing Organization Name and Address McCormick School of Engineering and Failure Prevention Northwestern University 2145 Sheridan Road Evanston, Illinois 60208				10. Work Unit No. (TRAIS)	
				11. Contract or Grant No.	
12. Sponsoring Agency Name and Address U.S. Department of Transportation FAA Los Angeles ACO 3960 Paramount Blvd Lakewood, CA 90712				13. Type of Report and Period Covered Final Report	
				14. Sponsoring Agency Code AIR-600	
15. Supplementary Notes The FAA William J. Hughes Technical Center Aviation Research Division COR was Dr. Felix Abali.					
16. Abstract In this report, the static strength of the aluminum D357-T6, sand-cast, Boeing 757 EE access door is assessed under several scenarios. These scenarios are encompassed by Title 14 Code of Federal Regulations (CFR) 25.621 for casting factors, CFR 25.305 for deformation and strength requirements, and CFR 25.603 and 25.613 for material properties requirements. Related activities in this research program include addressing casting process simulation, non-destructive evaluation process simulation, integrated design methodologies, and damage tolerance assessment of cast structures.					
17. Key Words Aluminum D357-T6, Sand-cast, Boeing 757 EE, Access door			18. Distribution Statement This document is available to the U.S. public through the National Technical Information Service (NTIS), Springfield, Virginia 22161. This document is also available from the Federal Aviation Administration William J. Hughes Technical Center at <a href="http://actlibrary.tc.faa.gov">actlibrary.tc.faa.gov</a> .		
19. Security Classif. (of this report) Unclassified		20. Security Classif. (of this page) Unclassified		21. No. of Pages 49	
				22. Price	

## ACKNOWLEDGEMENTS

We are grateful for the support of the FAA and the guidance provided by Drs. Xiaogong Lee, John Bakuckas, and Felix Abali of the William J. Hughes Technical Center; and Dr. Terry Khaled of FAA NRS Longbeach. Input from Ed Nichols, Vought Aerospace; Ed Costello and Ted Reinhardt, The Boeing Company; Joe Asada, Ryobi Limited Group of Companies; and from all our industrial advisors and collaborators is greatly appreciated.



## TABLE OF CONTENTS

	Page
EXECUTIVE SUMMARY	VIII
1. INTRODUCTION	1
1.1 Purpose	1
1.2 Background	1
1.3 Related Documents	2
2. OBJECTIVE	3
3. TECHNICAL APPROACH	3
3.1 Stress Analysis of the Casting	3
3.1.1 Introduction	3
3.1.2 The Boundary Value Problem of the Boeing 757 EE Access Door	4
3.1.3 Modeling the Stop Region	5
3.1.4 Stress Analysis Results for the Boeing 757 EE Access Door	8
3.1.5 Supporting Benchmark Problems	8
3.1.6 Results	17
3.1.7 Static Strength Assessment of the Casting	29
4. CONCLUSION	37
5. REFERENCES	38

## LIST OF FIGURES

Figure	Page
1 Integrated approach to design and quality assurance of premium quality aerospace castings	2
2 Boundary conditions for Boeing 757 EE access door in various models	4
3 Loading condition, uniform pressure (9 psi = 62 MPa) applied on the top surface of the door	5
4 Mesh of the stop region before and after being linked with the shell elements	6
5 The 270,000 DOF model for the Boeing 757 EE access door casting	6
6 Evolution of the stop region modeling	7
7 Clamped beam under a uniform pressure	9
8 Displacement results of the clamped beam	10
9 Bending of a plate modeled with shell and continuum elements (mesh)	11
10 Bending of a plate modeled with shell and continuum elements	13
11 Bending of a plate modeled with shell and continuum elements (error norm)	14
12 Displacement results for rod in tension modeled using MPC elements	15
13 Stress results for rod in tension modeled using MPC elements	15
14 Energy error norm results for a rod in tension modeled using MPC elements	16
15 Von Mises stress values in the stop region (mN/mm <sup>2</sup> )	18
16 Comparison of stress results in the stop region for three models	20
17 Displacement results in the casting	21
18 Deformed shape of the casting in the stop region (amplification factor of 500)	22
19 Comparison of displacement values in the Boeing 757 EE access door casting for two models	23
20 Displacement results in the stop region of the Boeing 757 EE access door casting for three models	24
21 Deformation in the Boeing 757 EE access door casting	25
22 Norm of error in the stress in the strut of the stop region for three models of the Boeing 757 EE access door casting	26
23 Norm of error in the continuum elements representing the stop region of the Boeing 757 EE access door casting	27
24 Comparison of the von Mises stress values far from the stop region for two models	28

## LIST OF TABLES

Table		Page
1	Casting factor quick guide: from design and specification of aluminum airframe structural castings	30
2	Tensile properties of the 1.25-inch-thick, water and glycol-quenched D357-T6 plates	31

## LIST OF ACRONYMS

AGARD	Advisory Group for Aerospace Research and Development
CF	Casting factor
DOF	Degrees of freedom
MMPDS	Metallic Material Properties Development and Standardization
MPC	Multiple point constraint

## 1. EXECUTIVE SUMMARY

This report summarizes a portion of the research and development activities carried out on FAA Contract DTFA03-98-F-IA025, “Design and Quality Assurance of Premium Quality Aerospace Castings Towards Assessing the Static Strength of the Boeing 757 EE Access Door.” The principal investigators on the project were Professors James G. Conley and Brian Moran, faculty members in the Center for Quality Engineering and Failure Prevention; Robert R. McCormick, School of Engineering and Applied Science, Northwestern University; and Mr. Stéphane Bordas, graduate student in Theoretical and Applied Mechanics, Northwestern University.

In this report, the static strength of the aluminum D357-T6, sand-cast, Boeing 757 EE access door is assessed under several scenarios. These scenarios are encompassed by Title 14 Code of Federal Regulations (CFR) 25.621 for casting factors, CFR 25.305 for deformation and strength requirements, and CFR 25.603 and 25.613 for material properties requirements.

Related activities in this research program include addressing casting process simulation, non-destructive evaluation process simulation, integrated design methodologies, and damage tolerance assessment of cast structures.

## 2. INTRODUCTION

### 2.1 PURPOSE

Airworthiness standards are governed by Title 14 Code of Federal Regulations. In particular, 14 CFR Parts 25 and 33 include airworthiness standards for transport category airplanes and aircraft engines, respectively. CFR Part 25 mandates that all primary structures of airframe component design must satisfy the principles of damage tolerance [1].

Castings must meet the same strength requirements as other wrought or assembled metallic structures (e.g., material characterization, static strength, durability, and damage tolerance). Of these four criteria, this report will examine static strength.

The variability of cast alloy material properties within a casting and across castings of the same configuration has hindered the establishment of statistically valid allowables. The so-called casting factor (CF), an additional factor of safety reducing the static design strength, was created to account for this uncertainty on material properties. In certain controlled instances, it is possible—with the agreement of the FAA—to reduce the CF to 1.0. Several critical D357-T6 structural castings and Ti-alloy airframe castings have been designed with a CF of unity [2–5].

Federal aviation regulations allow that material data used in design be taken from the Metallic Material Properties Development and Standardization (MMPDS) Handbook [6]. Note that this standard is the current embodiment of what has historically been referred to as MIL-HDBK-5.

The first step in the qualification process of an aeronautical component is static strength assessment. This report discusses the various factors, margins, and material property values (allowables) that should be accounted for in this assessment [7–99].

### 2.2 BACKGROUND

Conley, Moran, and Gray [10] proposed a new integrated approach to the design of safety-critical castings, such as airframe components (see figure 1). This approach shows promise for evaluating the damage tolerance and fail safety of a given structural component using computer simulation methods to improve design efficiency. The method employs: 1) a foundry process simulation to predict cast defects and imperfections, 2) crack growth modeling methods to predict the effect of said defects on fatigue life and residual strength, and 3) modeling of nondestructive evaluation processes to determine the inspectability of both initial defects and potential cracks that may grow in service. However, an assessment of the static strength of a casting must first be made before assessing damage tolerance and durability of that casting.

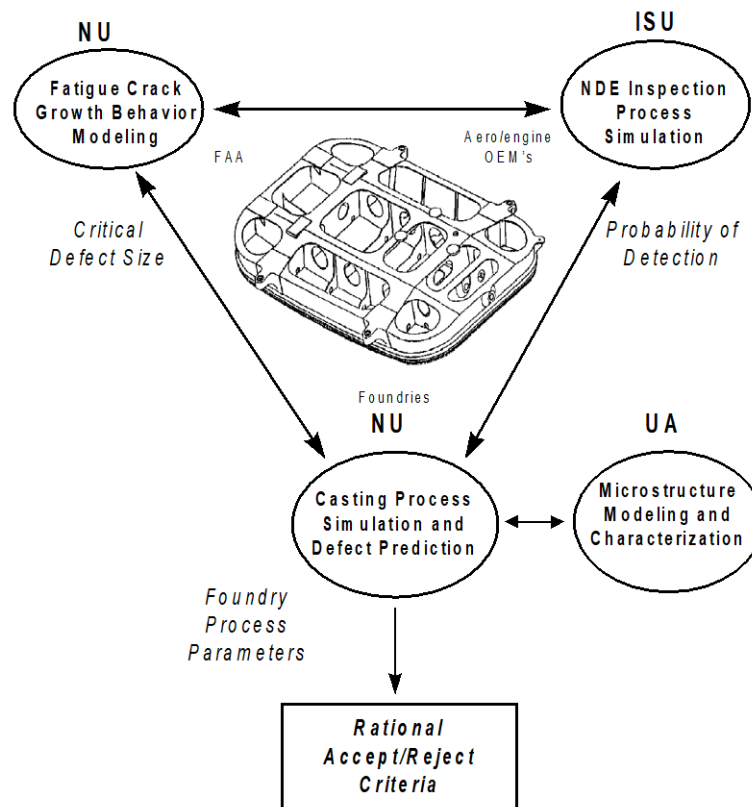


**Figure 1. Integrated approach to design and quality assurance of premium quality aerospace castings**

Related aspects of this research program pertaining to the stress analysis of the approach are described through application to a Boeing 757 EE access door. In particular, several finite element models of the door are described and their results compared. Different scenarios using adaptive meshing techniques are chosen to depict the behavior of the handle region. This and the stop regions (locations to be explained in section 3.1.2.1) are of interest because finite element models of the door show that they exhibit the highest stress values. Difficulties in modeling continuum shell interfaces are noted and remedies proposed and implemented. Those remedies ensure an accurate and reliable assessment of the component and provide a starting point for the static strength assessment.

## 2.3 RELATED DOCUMENTS

The following documents relate directly to the static strength analysis addressed in this report.

1. 14 CFR Parts 25 and 33 are airworthiness standards for transport category airplanes and aircraft engines, respectively. 14 CFR 25 mandates that all primary structure airframe component design must satisfy the principles of damage tolerance [1].
2. The Defense Technical Information Center publications from the Defense Information Systems Agency reported various facts pertaining to casting factors (i.e., reports from the

Advisory Group for Aerospace Research and Development [AGARD]). The main report used here is AGARD's Report No.762, "Casting Airworthiness" [11].

3. The AGARD handbook on advanced castings [12].

### 3. OBJECTIVE

The objective of this report is to describe the approach used for the stress analysis and static strength assessment of the Boeing 757 EE access door. This will form the basis for subsequent work on damage-tolerance assessment.

This report addresses the following main points:

4. Stress analysis techniques for complex components that implement solid and shell elements for the Boeing 757 EE access door
5. Discussion of CF, material properties databases, and CFR for design of structural castings
6. Static strength assessment of the casting under CFR
7. Design recommendations for the selected casting

### 4. TECHNICAL APPROACH

#### 4.1 STRESS ANALYSIS OF THE CASTING

##### 4.1.1 Introduction

The stress analysis of the Boeing 757 EE access door is described in this section. It was estimated that a full continuum model of the door with several solid elements through the thickness of thin struts and skin would lead to a problem with approximately 20 million degrees of freedom, which is computationally prohibitive. To reduce the problem size, the door was modeled using Bathe-Dvorkin [13–14] Mindlin Reissner shell elements for the thin parts, such as the skin and struts; continuum tetrahedral elements were used for the thicker parts, such as the stop regions. Spurious stress concentrations associated with the transitions from continuum to shell elements are addressed.

In particular, the continuum elements used to model the stops were continued into the door to drive the stress concentrations associated with the transition from continuum to shell elements away from the filleted region, where the stop was attached to the door. This ensured that the spurious stress concentrations occurred in a region of relatively uniform stress. This made it possible to obtain the stresses in those regions by other approaches and to estimate the magnitude of the spurious concentrations.

Shell elements and solid elements were linked using multiple point constraint (MPC) elements. Several benchmark problems are presented to demonstrate the performance of the MPC elements in linking shell and tetrahedral meshes to support and explain the results obtained for the Boeing 757 EE access door.



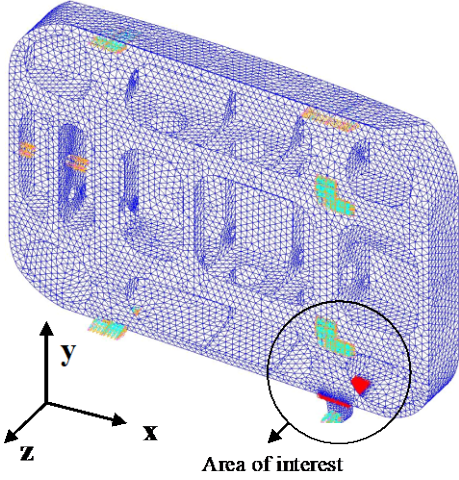
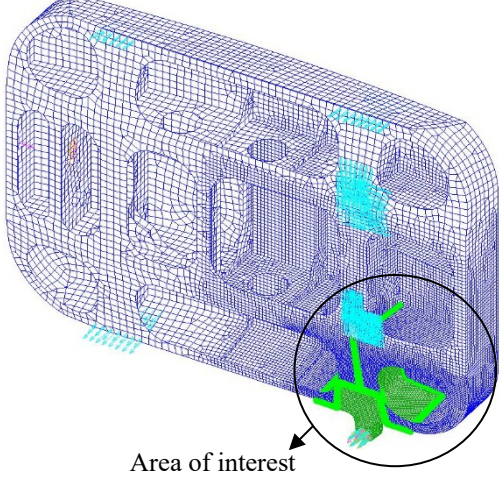
## 4.1.2 The Boundary Value Problem of the Boeing 757 EE Access Door

### 4.1.2.1 Boundary Conditions

The displacement boundary conditions used in the analysis are the following:

- $z$  direction displacement restraints:
  - Cylindrical hole in the stop is fixed in the  $z$  direction.
  - Shell nodes located at the footprint of the stop are fixed in the  $z$  direction areas, where the stops are not explicitly modeled.
- $x$ - $y$  direction displacement restraints:
  - Nodes are fixed in  $x$  and  $y$  directions at the location of the hinged arm on the back surface of the door.
  - Nodes at the location where the latch pin interacts with the door are fixed in the  $x$  direction.

Figure 2 shows the applied displacement boundary conditions on the casting models used for the stress analysis.

Stop modeled using linear tetrahedrons linked to linear shells with rigid elements	Stop modeled with quadratic tetrahedrons linked to linear shells with MPC elements
	

**Figure 2. Boundary conditions for Boeing 757 EE access door in various models**

It is important to note that different stress values would be obtained if the boundary conditions were implemented differently, such as through the restraint of the outer surface of the stop in the  $z$  direction. However, the stress field in the stop region is expected to be close to that reported.

#### 4.1.2.2 Loading

The loading condition, as shown in figure 3, was taken to be the normal operating pressure of 62 MPa (9 psi = 8.6 + 0.4 psi for external dynamics error). This pressure was taken to be the limit load for the static strength assessment of the component. Temperature effects were not accounted for in the present calculation.

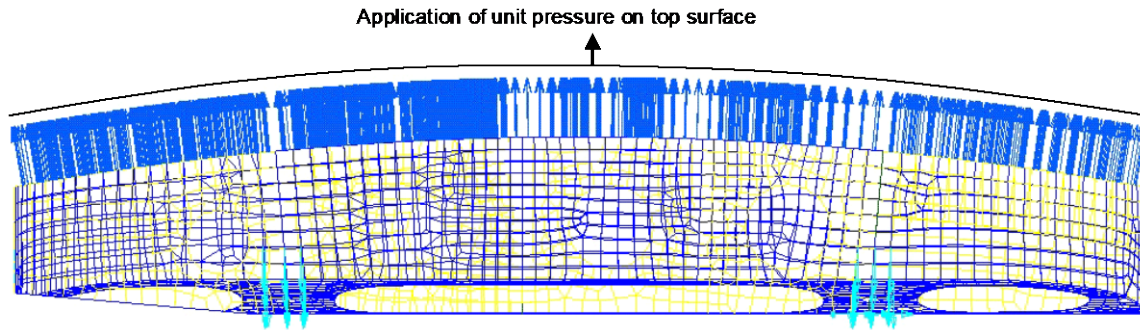


**Figure 3. Loading condition, uniform pressure (9 psi = 62 MPa) applied on the top surface of the door**

#### 4.1.2.3 Material Properties

The material properties used for the D357-T6 aluminum were 72.4 GPa for the modulus of elasticity ( $E$ ) and 0.33 as the Poisson's Ratio ( $\nu$ ). The shear modulus  $G$  was computed from  $G = E/2(1+\nu)$  and is equal to 27.2 GPa.

#### 4.1.3 Modeling the Stop Region

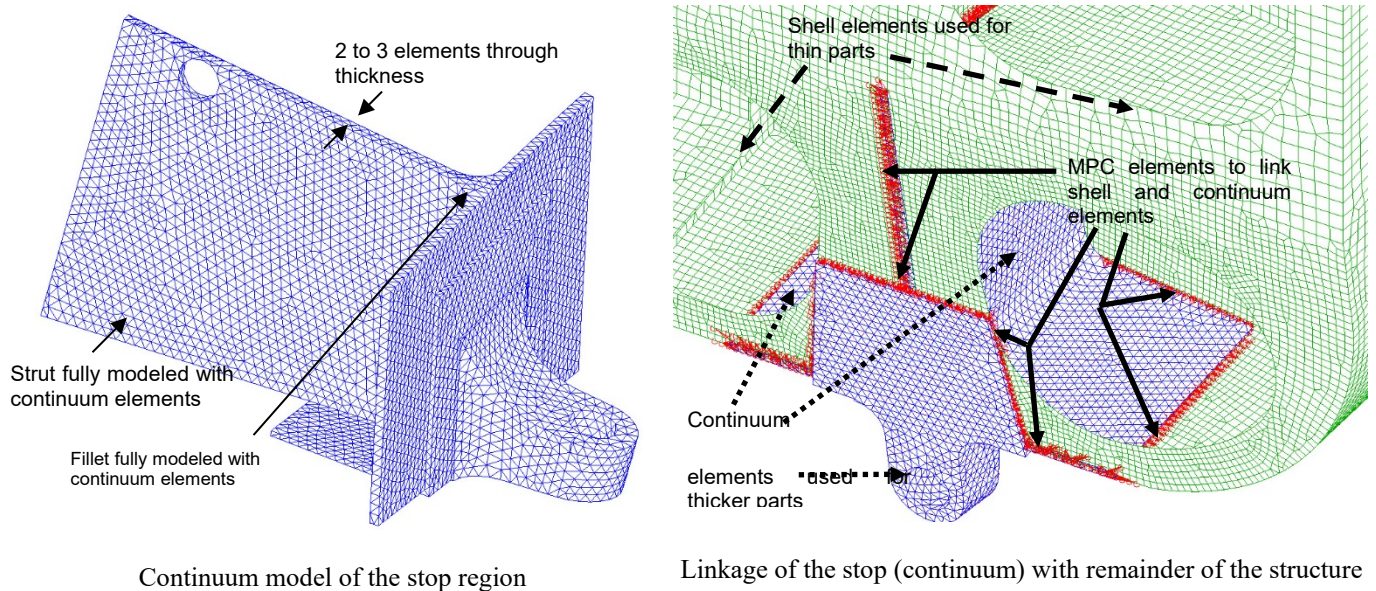
It has been shown [9] that Mindlin Reissner shell elements accurately and efficiently modeled the behavior of the thin structural components of the door. However, the stops through which the door was restrained from being pulled out of the aircraft are thick structures that cannot be modeled using shell elements.

One possibility to model the stop region consists of building a solid model for the stops and attaching them with rigid elements to the shell model of the remainder of the door. This technique is unsatisfactory because it creates spurious stress concentrations as high as 150 MPa at the interface between continuum and shell elements.

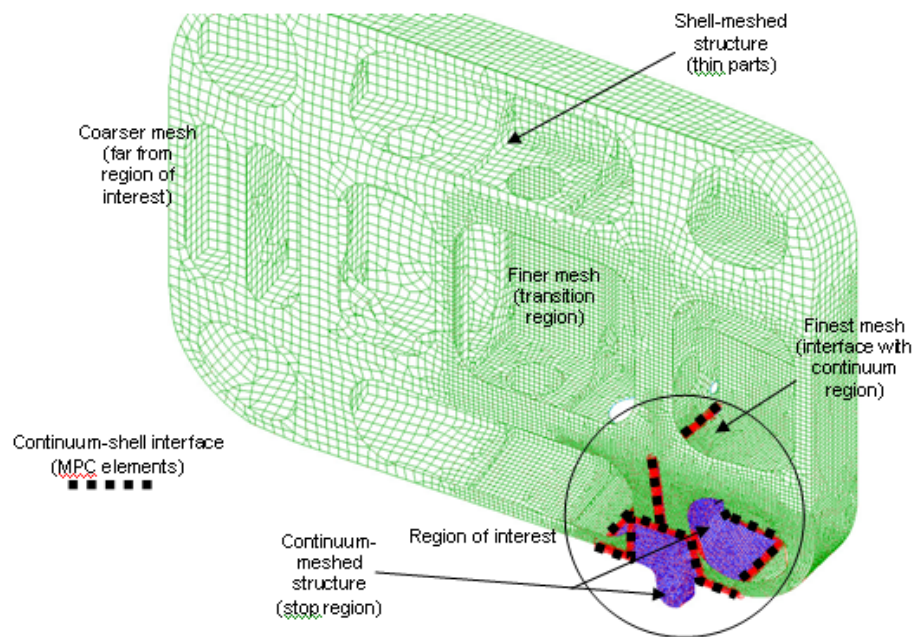
To accurately compute the stress values in the stop region, a full continuum model of the region was created using EDS-PLM/I-DEAS (formerly SDRC/I-DEAS) solid modeling software. As shown in figure 4, the continuum region is continued from the stop well into the door. The strut was fully modeled with solid elements, to include the fillet and wall thickness gradient. The stop mesh shown in figure 5 is composed of 31,812 quadratic tetrahedral elements, which are significantly less stiff than linear tetrahedral elements and give more accurate results for the same level of discretization. Only one stop region was modeled in detail because the structural behavior



of the door in all four stop regions is very similar. The other stops were not included in the model and their influence was accounted for by restraining the shell nodes at the attachment location.



**Figure 4. Mesh of the stop region before and after being linked with the shell elements**

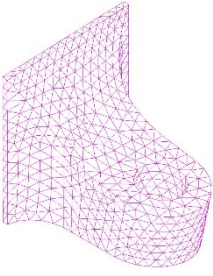
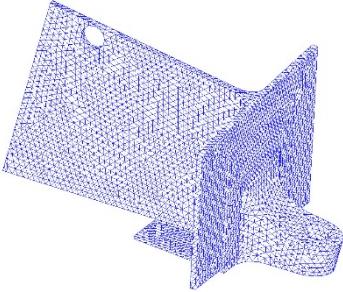
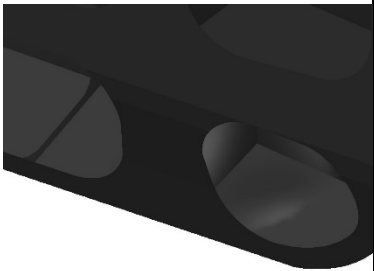
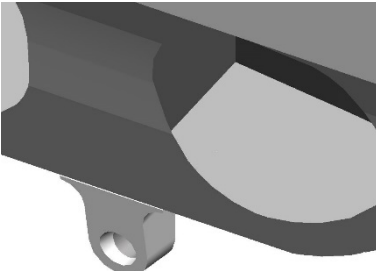
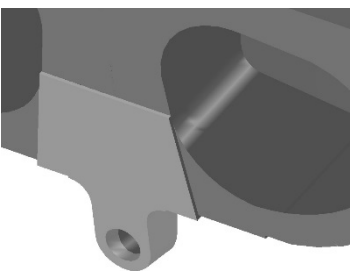
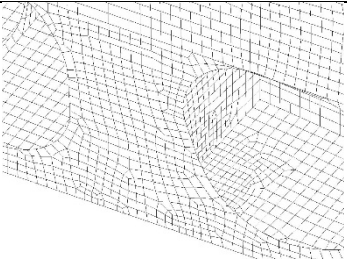
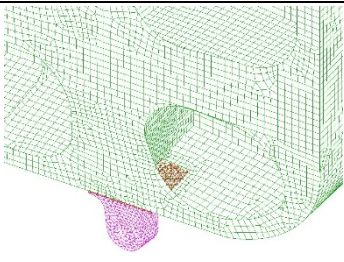
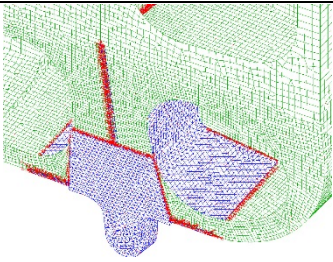


**Figure 5. The 270,000 DOF model for the Boeing 757 EE access door casting**

The mesh of the stop is linked to the surrounding shell elements using MPC elements (see figure 5). Those elements, as opposed to rigid elements, are known to lead to smaller stress concentrations at shell and continuum interfaces. The nodes of the tetrahedral elements that have

one face on the boundary of the continuum-meshed domain are linked to the shell elements, which have one edge aligned with the corresponding edge of the shell-meshed geometry. The influence of the three rotational degrees of freedom (DOF) at the shell nodes is therefore transmitted to the tetrahedral elements by enforcing a linear constraint equation relating the value of their DOF to those of the associated continuum nodes.

To reduce computational costs, the shell mesh was gradually refined with 10 mm elements as it approached the stop region from remote locations and 2 mm elements at the interface with the stop. The Boeing 757 EE access door's stop and its surrounding region are shown in figure 6.

	Fixed nodes at the attachment of the stops to the door	Stop modeled and linked using rigid elements to the shell surface	Stop region fully modeled including the strut and filleted area
Stop model	NA		
Stop region			
Mesh of stop region			

**Figure 6. Evolution of the stop region modeling**

Note that the use of MPC elements to interface continuum elements with shell elements is not an exact technique. Sections 3.1.5 and 3.1.6.4 show that the largest computed error in the model occurred at this interface. Also, although MPC elements tend to have a more compliant behavior than rigid elements, unrealistically high stress values were observed at the interface. However, if

this interface is located far enough from the region of interest, the application of this technique does not lead to excessive loss in accuracy. Because previous analyses gave reasonable stress values for the component, except in the stop region, the interface was placed away at a location where there were reliable stress values obtained through other models.

Figure 6 shows the evolution of the solid and finite element modeling of the stop region. The current model is depicted in the rightmost column.

#### 4.1.4 Stress Analysis Results for the Boeing 757 EE Access Door

##### 4.1.4.1 Stress Measures

The stress and strain measures used in displaying results are the von Mises effective stress and strain given by:

$$\bar{\sigma} = \sqrt{\frac{3}{2} s_{ij} s_{ij}} \quad \bar{\epsilon} = \sqrt{\frac{2}{3} e_{ij} e_{ij}} \quad (1)$$

$$s_{ij} = \sigma_{ij} - \frac{1}{3} tr(\boldsymbol{\sigma}) \delta_{ij} = \sigma_{ij} - \frac{1}{3} \sigma_{kk} \delta_{ij} \quad (2)$$

$$e_{ij} = \epsilon_{ij} - \frac{1}{3} tr(\boldsymbol{\epsilon}) \delta_{ij} = \epsilon_{ij} - \frac{1}{3} \epsilon_{kk} \delta_{ij} \quad (3)$$

where:  $s_{ij}$  is the deviatoric stress and  $e_{ij}$  is the strain tensors, and  $\sigma_{ij}$   $\epsilon_{ij}$  are the stress and strain tensors, respectively;  $\delta_{ij}$  is the unit second-order tensor, and summation over repeated indices is implied.

In addition to the von Mises stress, the maximum principal stress and shear stress are also reported and analyzed. Unless otherwise specified, all stress values are given in MPa and displacements in millimeters.

#### 4.1.5 Supporting Benchmark Problems

In this section, three benchmark problems that give insight on the behavior of MPC elements are examined:

1. A beam bending problem in which the center part of the beam was replaced with a mesh of tetrahedral elements linked to beam elements using MPC elements
2. A plate bending problem in which the center part of the plate was replaced with a mesh of tetrahedral elements linked to the shell elements using MPC elements

3. A rod under uniaxial tension in which the meshed rod with tetrahedral elements was artificially cut into two pieces and linked by MPC elements

These problems prove that MPC elements can be successfully used to join dissimilar meshes and that the error introduced by the linking process is localized in the interface region between the two meshes.

#### 4.1.5.1 Beam/Continuum Interface Using MPC Elements

The beam is clamped at both ends and subjected to a uniform unit pressure (see figure 7). The same problem was also solved using only beam elements. The displacement results in the beam for both methods are compared in figure 8.

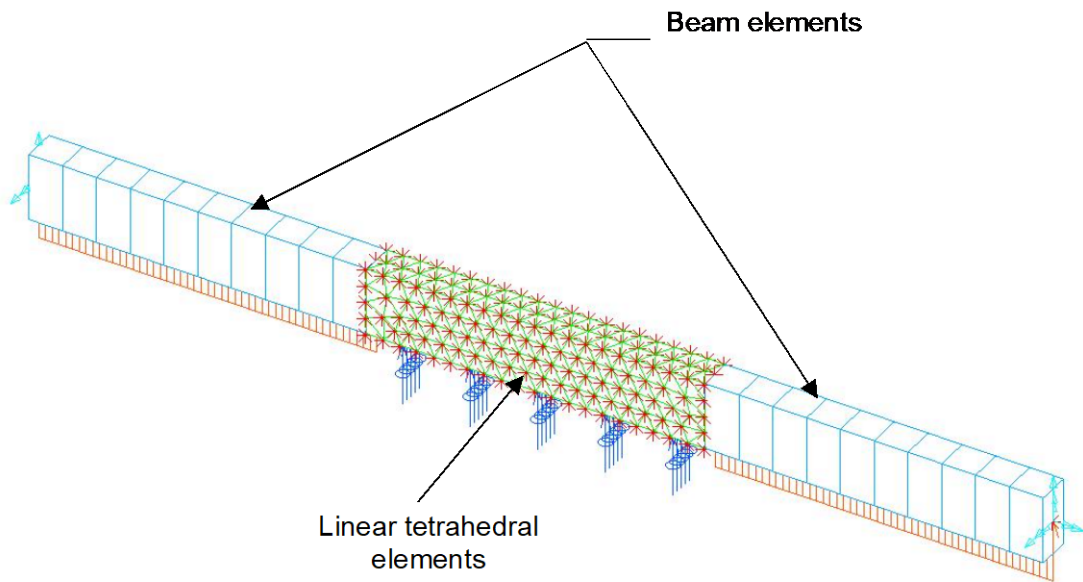


**Figure 7. Clamped beam under a uniform pressure (center part was modeled using continuum elements)**



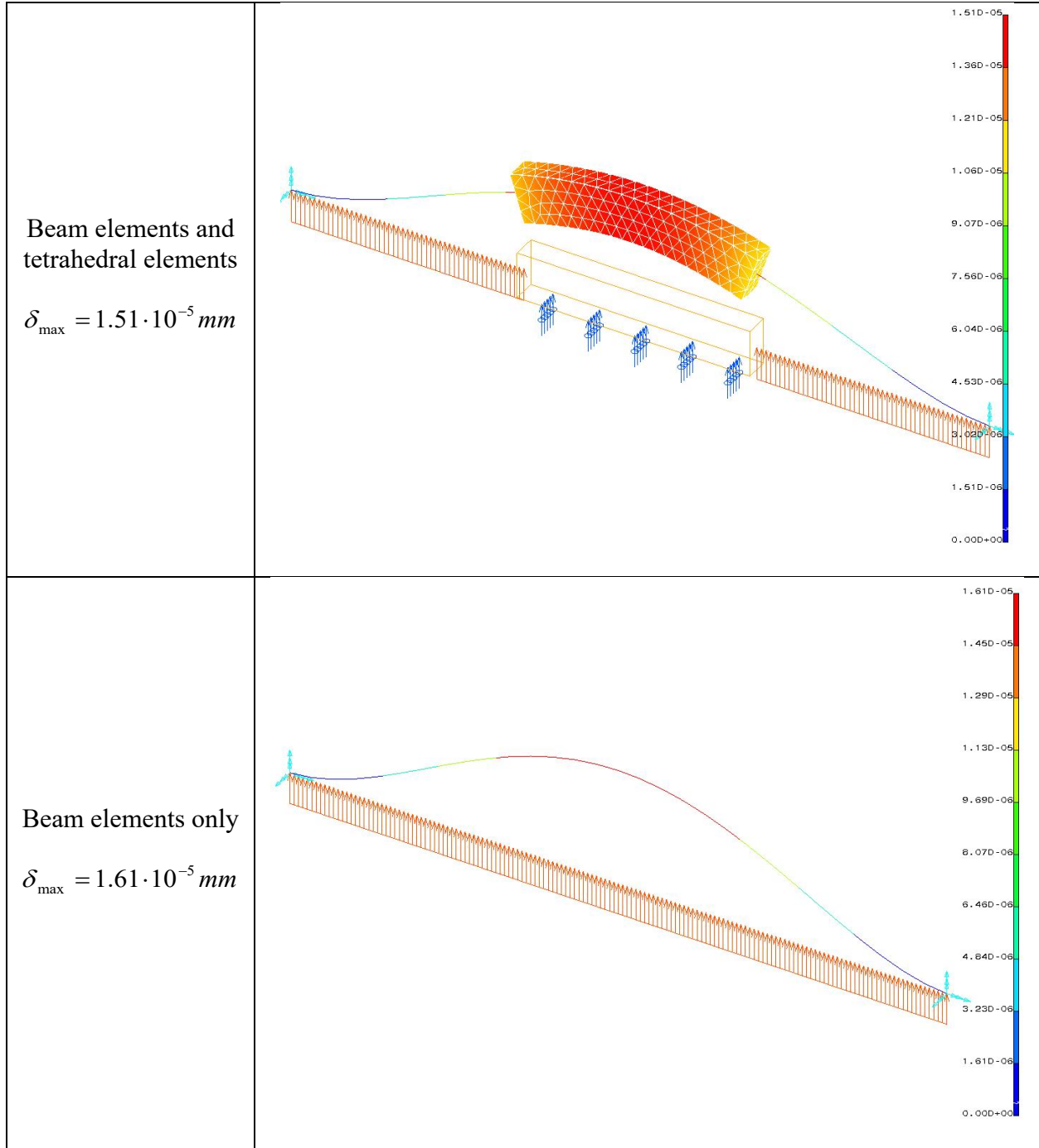


**Figure 8. Displacement results of the clamped beam**

Good agreement was observed in the displacement results with a relative error of only 6%. This verifies that the rotations of the beam elements were accurately transferred to the tetrahedral elements. The error could be further reduced by using quadratic tetrahedral elements for the central part. Also, note that four tetrahedral elements were used through the thickness of the beam to capture the bending behavior.

#### 4.1.5.2 Shell/Continuum Interface in Bending

In figure 9, a plate-bending problem is shown. The central part of the plate is modeled with linear tetrahedral elements, which are linked to shell elements in the remaining portion of the plate using the MPC elements. The plate is clamped on the right end and subjected to a uniform unit pressure.

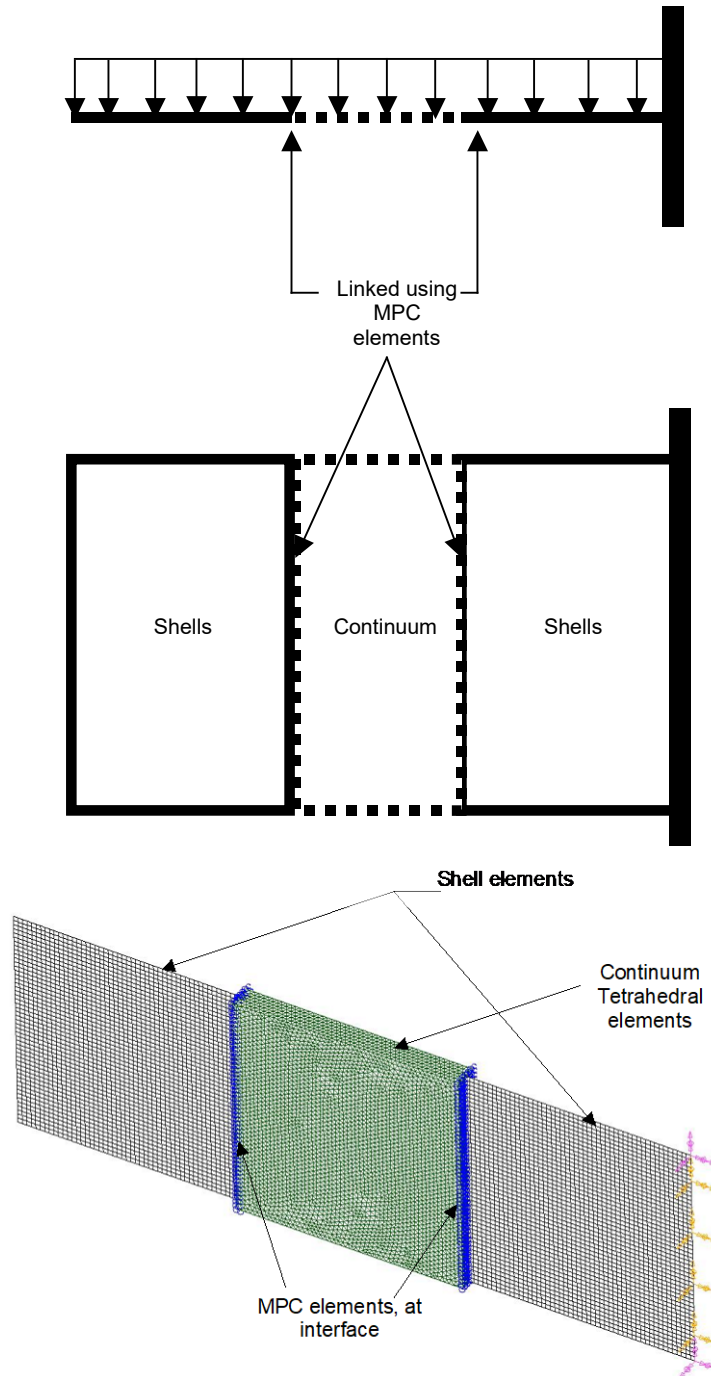


**Figure 9. Bending of a plate modeled with shell and continuum elements (mesh)**



As shown in figure 10, the MPC elements provided a correct enforcement of displacement continuity through the shell/continuum interface. Also, the relative error in displacement is less than 2% everywhere in the domain and approximately 2% at the left (free) end of the plate. The difference in the stress value is very small in locations far from the shell/continuum interface and the Dirichlet boundary (right end of the plate). However, the maximum stress at the clamped end of the plate is overestimated by 17%. This is because the right clamped end of the plate experienced mixed boundary conditions (Dirichlet from the clamped restraint and Neumann from the applied pressure), which are known to cause singularities. In fact, there exists a point load type singularity at the right edge of the plate, and refining the mesh only leads to greater values without convergence. This is a typical case in which the finite element method fails to converge to a solution. In addition, whereas the displacement field is continuous and accurate close to the shell/continuum boundary, the stresses field is erroneous. Therefore, the shell/continuum interface is moved away from the region of interest to maintain accurate stress values.

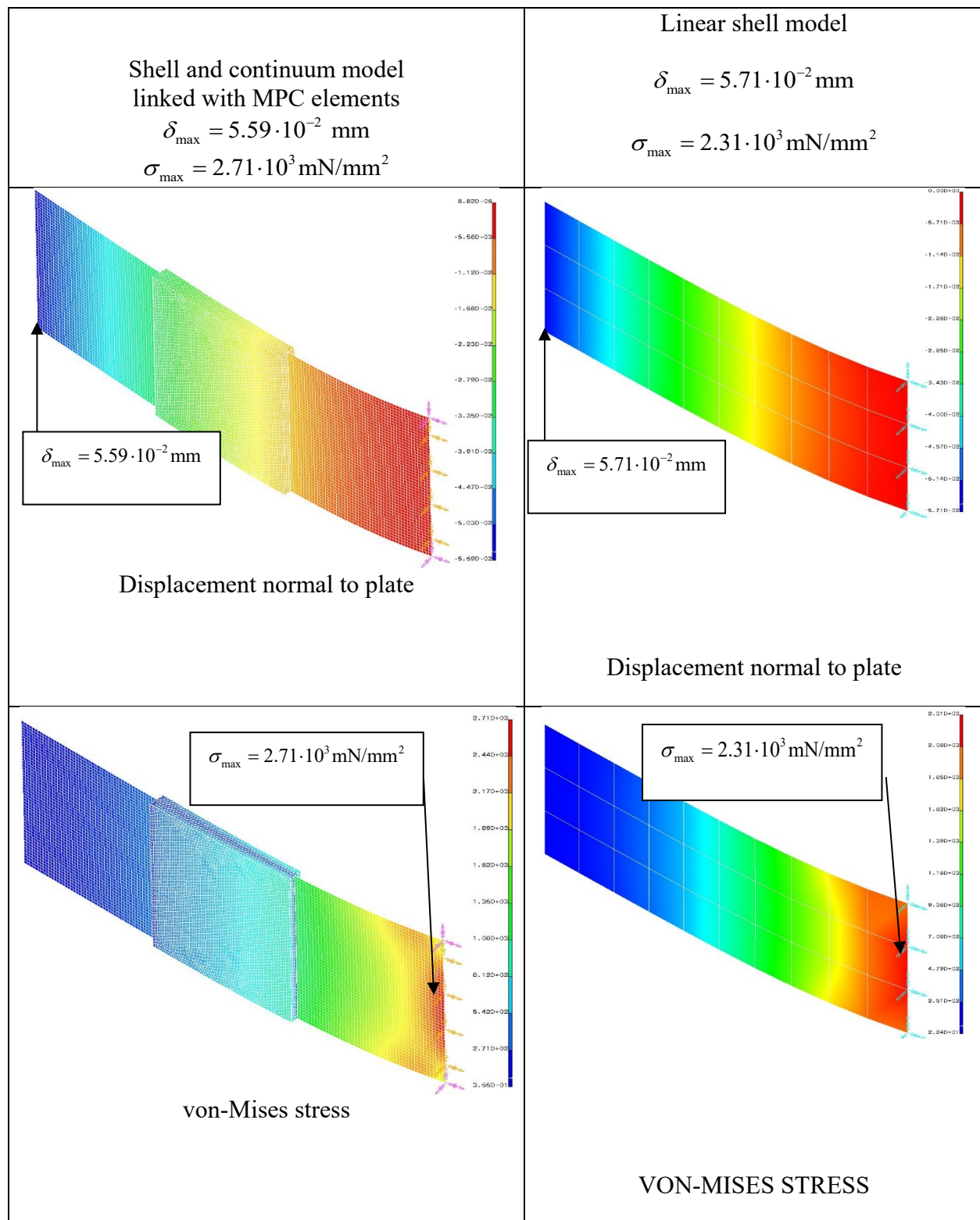


**Figure 10. Bending of a plate modeled with shell and continuum elements (displacement and von Mises stress)**

Comparing results of the models in figure 10, the rotations of the shell elements were accurately transferred to the continuum elements. The displacements are more accurate than the stresses at the location where the stop is linked to the door with MPC elements. The displacements are obviously more accurate than stresses at the location. Also, it is interesting to note that the error in the approximation is concentrated at the interface between continuum and shell elements. This is also the case in the model of the Boeing 757 EE access door and in the other benchmark problems presented in this section. Note also that when MPC elements are replaced with rigid elements in the analysis shown in this section, similar results are reported with a maximum stress of  $\sigma_{\max} = 2.65 \cdot 10^3 \text{ mN/mm}^2$  and a maximum displacement of  $\delta_{\max} = 5.40 \cdot 10^{-2} \text{ mm}$ .

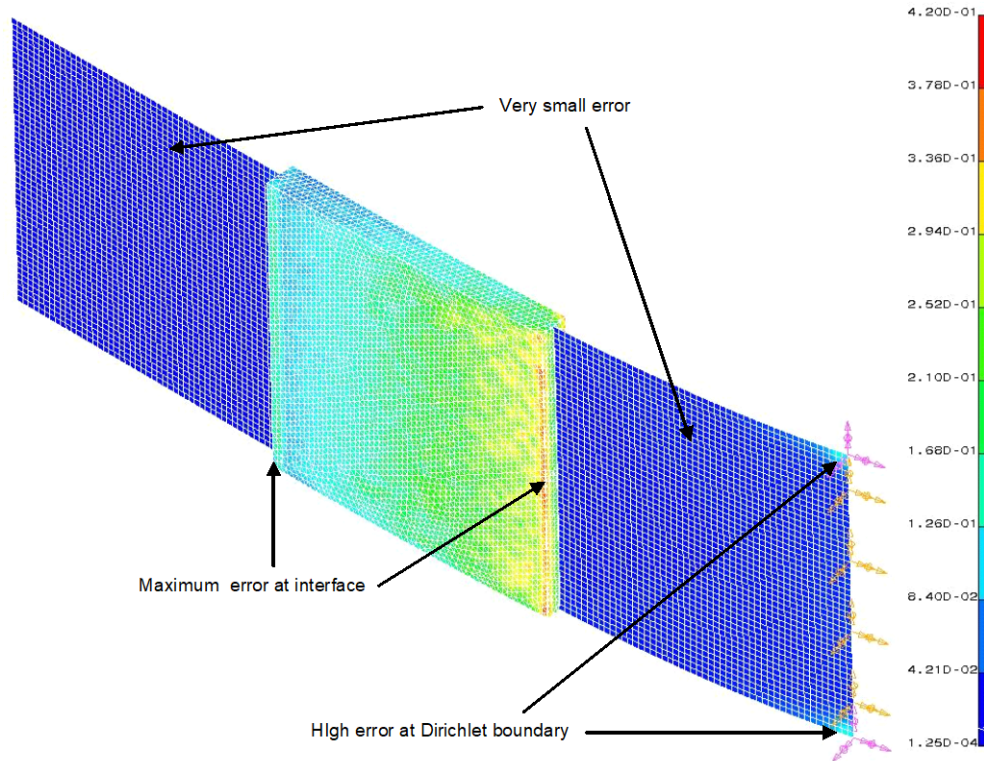


**Figure 11. Bending of a plate modeled with shell and continuum elements (error norm)**

#### 4.1.5.3 Continuum/Continuum Interface of a Rod in Tension

In this benchmark, displacement and stress results for a rod ( $E = 1 \text{ mN/mm}^2$ ,  $\nu = 0$ ) under uniaxial tension are compared for two different models:

1. All quadratic tetrahedral elements
2. Linear tetrahedral elements linked by MPC elements

The rod has a 10 mm by 10 mm square section and is 40 mm long. It is sufficiently restrained at end B and subjected to a uniform traction of  $1 \text{ mN/mm}^2$  at end A. The stress in the rod is constant and equal to  $1 \text{ mN/mm}^2$ ; the maximum displacement occurs at end A of the rod and is exactly 40 mm, which is the analytical solution given by the theory of linear elasticity.

Displacement results for both cases are shown in figure 12, and stress results are shown in figure 13 for the second case.

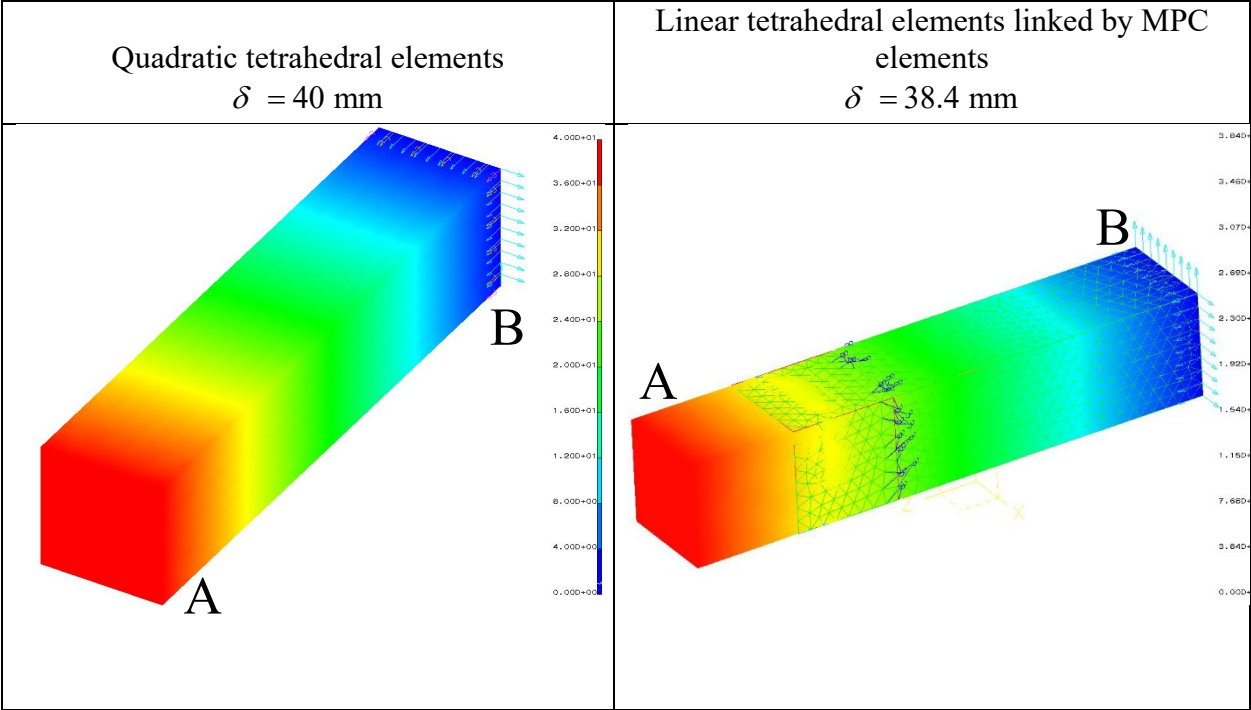


Figure 12. Displacement results for rod in tension modeled using MPC elements

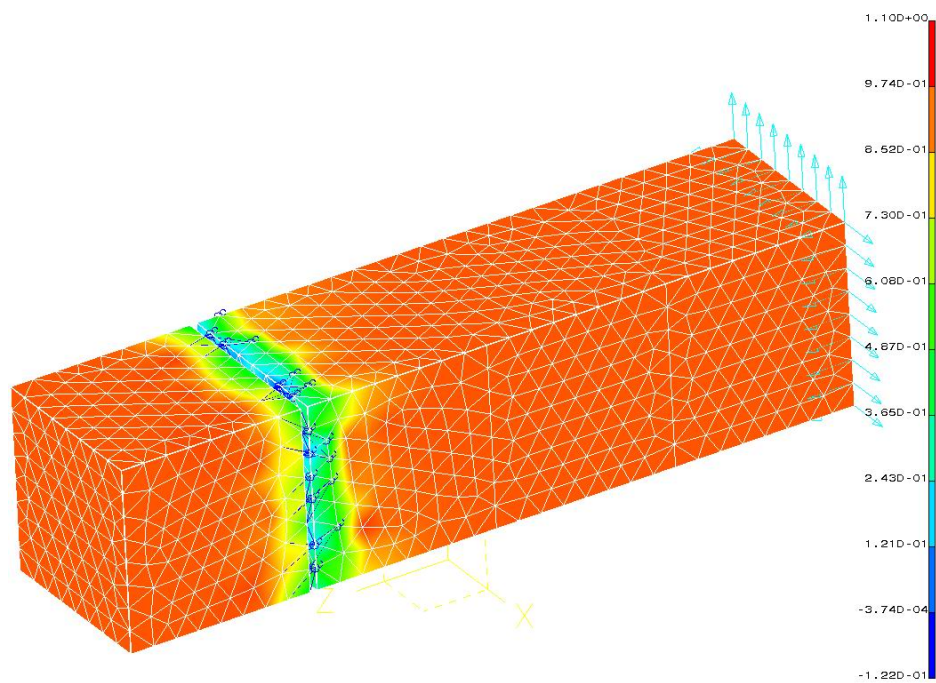
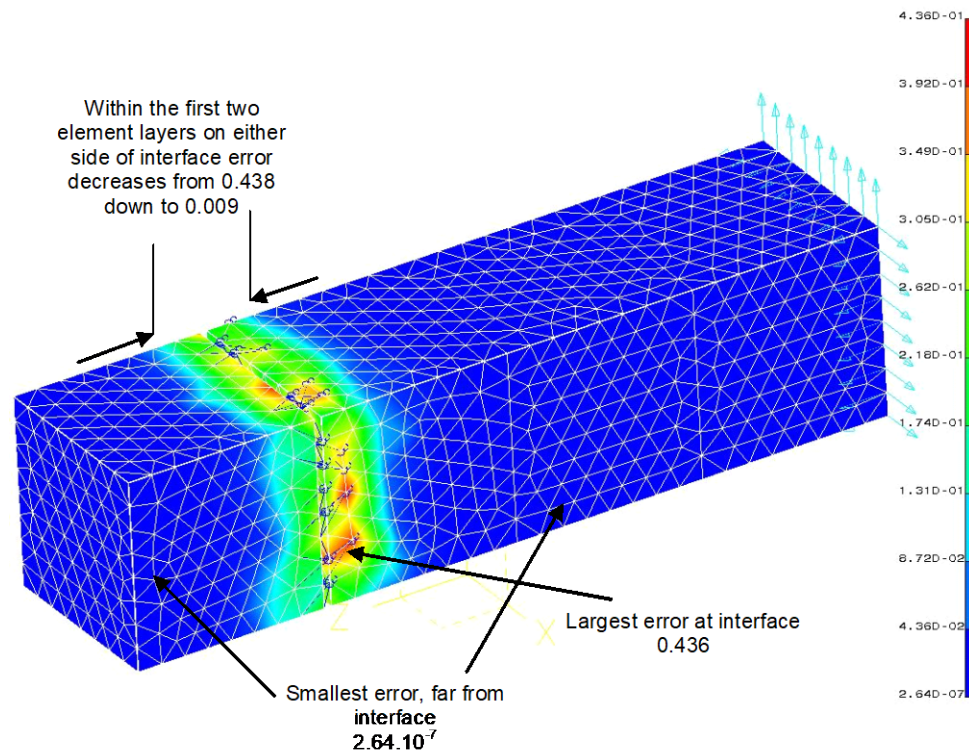


Figure 13. Stress results for rod in tension modeled using MPC elements



As shown in figure 13, the displacement at the end for the quadratic tetrahedral element model is exactly 40 mm. However, when using the MPC elements to link the portions of the rod, the maximum displacement is 38.4 mm, which represents a 4% relative error. The stress in the rod when using MPC elements is  $1.10 \text{ mN/mm}^2$ , which is 10% more than the exact value. The energy error norm values are shown in figure 14. The error is concentrated in the two layers of tetrahedrons immediately located on both sides of the interface where the MPC elements are used to enforce the constraints. It is also interesting to note that the energy error norm decreases by three orders of magnitude within the first three layers of elements and by another four orders of magnitude within the fourth layer from the interface in each direction. Starting at the fourth layer of elements on either side of the interface, the error reaches a constant value equal to  $2.64 \cdot 10^{-7}$ . The same behavior is noted when MPC elements are used to link the tetrahedral elements of the stop to the shell elements of the thin parts of the Boeing 757 EE access door casting. Note also that the use of quadratic tetrahedral elements in the case of the rod would also have decreased the energy error norm significantly. This is the reason why quadratic tetrahedral elements were used instead of linear elements to model the door casting.



**Figure 14. Energy error norm results for a rod in tension modeled using MPC elements**

From the benchmark problems previously described, the following conclusions can be drawn concerning the use of MPC elements for finite element models in which dissimilar meshes must be joined:

1. MPC elements succeeded in transmitting rotational DOF from shell and beam elements to continuum elements, such as tetrahedral elements.
2. In bending problems, it is important that the continuum element mesh is dense enough for structural compliance.
3. Errors in displacements were approximately a few percent, depending on the analysis.
4. Errors in stress were approximately 10%, and the stresses were always overestimated, never underestimated.
5. In the example showing the uniaxial tension of a rod, the error norm in energy decreases by three orders of magnitude within the first three layers of elements. It decreases by four more orders of magnitude in the fourth layer of elements.
6. The same behavior was observed in using MPC or rigid elements for the problems addressed in this work.

In particular, it was noted that, although the MPC is an approximate mesh transition technique, the stress results obtained were overestimated (i.e., MPC elements will give conservative results).

The results of the stress analysis of the Boeing 757 EE access door D357-T6 aluminum alloy casting are examined in the following section. In the current finite element model of the door, MPC elements were used to join continuum and shell elements. The benchmark problems of this section demonstrated that employing MPC elements in stress analyses is an adequate technique if stresses at the interface are not of primary importance.

#### 4.1.6 Results

In this section, the overall displacement, stress, and error norm results of the access door are compared with those obtained by other analyses, with the stop region modeled in less detail.

##### 4.1.6.1 Stresses in the Stop Region

Figure 15 shows the stress values at different locations in the stop region.

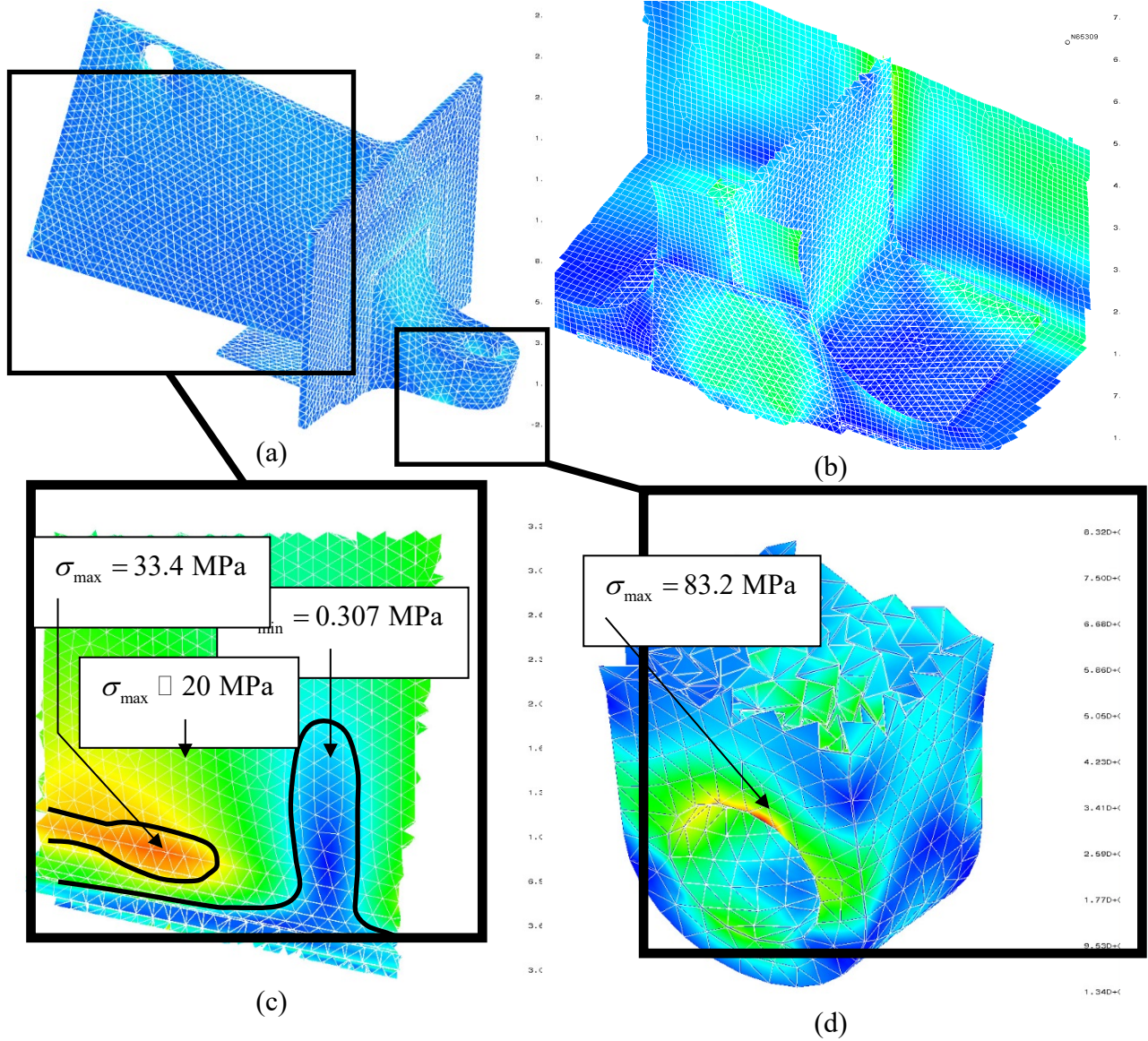


**Figure 15. Von Mises stress values in the stop region mN/mm<sup>2</sup>**

Note that the highest stress value (83.2 MPa in figure 15c) was obtained at the boundary condition nodes, where most of the pressure load ( $z$  component) is transmitted to the door. In the approximation of the restraint in the  $z$  direction, only nodes on the surface of the hole in the stop are fixed. This is a stiff way to enforce Dirichlet boundary conditions and is known to lead to singularities. A more compliant application of boundary conditions are expected to lead to lower stress values in the stop's hole region. Therefore, it is expected that the fairly high stress value of 83.2 MPa reported in the hole region is a result of the boundary condition modeling technique.

More advanced modeling of the stop boundary conditions should be used if the stress values in the hole region are to be evaluated with a higher accuracy. Modeling the restraint conditions at the stops in detail involves substantial modeling difficulties. The loads are transmitted from the stop to the fuselage through a bolted link. For an accurate modeling of the boundary conditions, the

bolts should be included in the model. An initial analysis could be performed using beam elements to model the bolt and link to the continuum elements through MPC elements. However, as shown in the benchmark problems presented in section 3.1.5.3, this would probably lead to spurious stress concentrations and large error in the bolt/stop interface. A more elaborate technique would be to fully model the bolt (with continuum elements similar to those of the stop), and explicitly model the contact between the two solids (the stop and the bolt). Contact algorithms are fairly complex numerical techniques that need to be calibrated, and the contact modeling capabilities of I-DEAS are insufficient to permit an accurate assessment of the behavior of the bolt/stop region. Moreover, because all the analyses performed using simplified boundary conditions are conservative (they lead to higher stress concentrations because of the point loads generated by the restraints), it was decided not to construct more elaborate models for the stop/fuselage interaction.

Figure 16 shows a comparison between the stress values obtained in this analysis and those obtained from previous analyses. Note that stresses in figure 16(C3) do not show any spurious concentration in the fillet region, as was the case in previous analyses—figures 16(C1) and 16(C2).



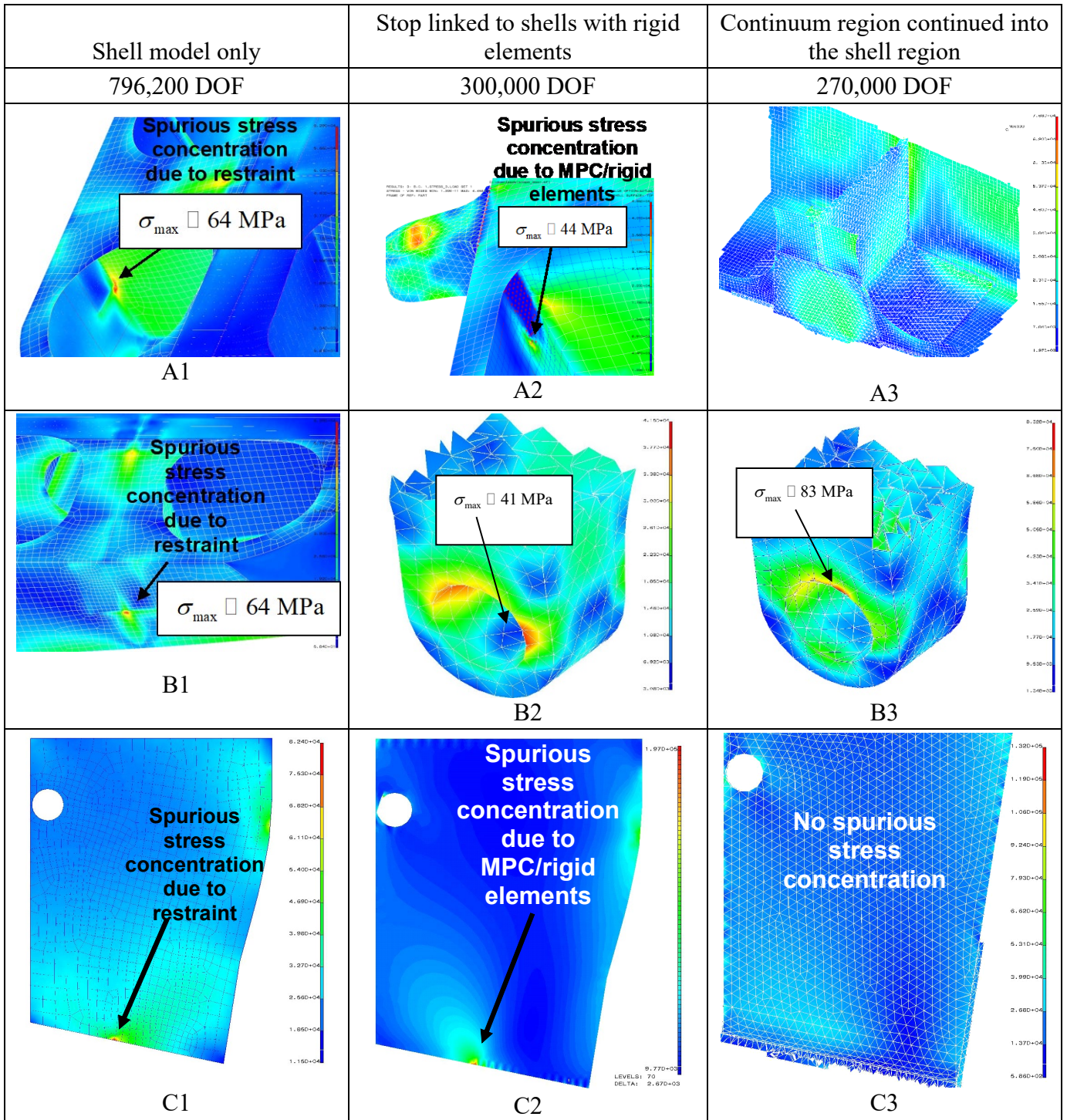


**Figure 16. Comparison of stress results in the stop region for three models**

#### 4.1.6.2 Displacement Field

Figure 17 shows the displacement results of the casting. The maximum calculated displacement is 0.987 mm and occurs in the handle region (figure 17(a)). The handle is modeled using the same

material properties as the rest of the structure. However, previous analyses showed that the type of material used for the handle in the model did not significantly affect the displacement results. Moreover, a stress value of 56.8 MPa is obtained when the handle is modeled as infinitely rigid. When the handle is modeled with aluminum material properties, the highest stresses (approximately 50 MPa) occur at the strut intersection on either side of the handle.

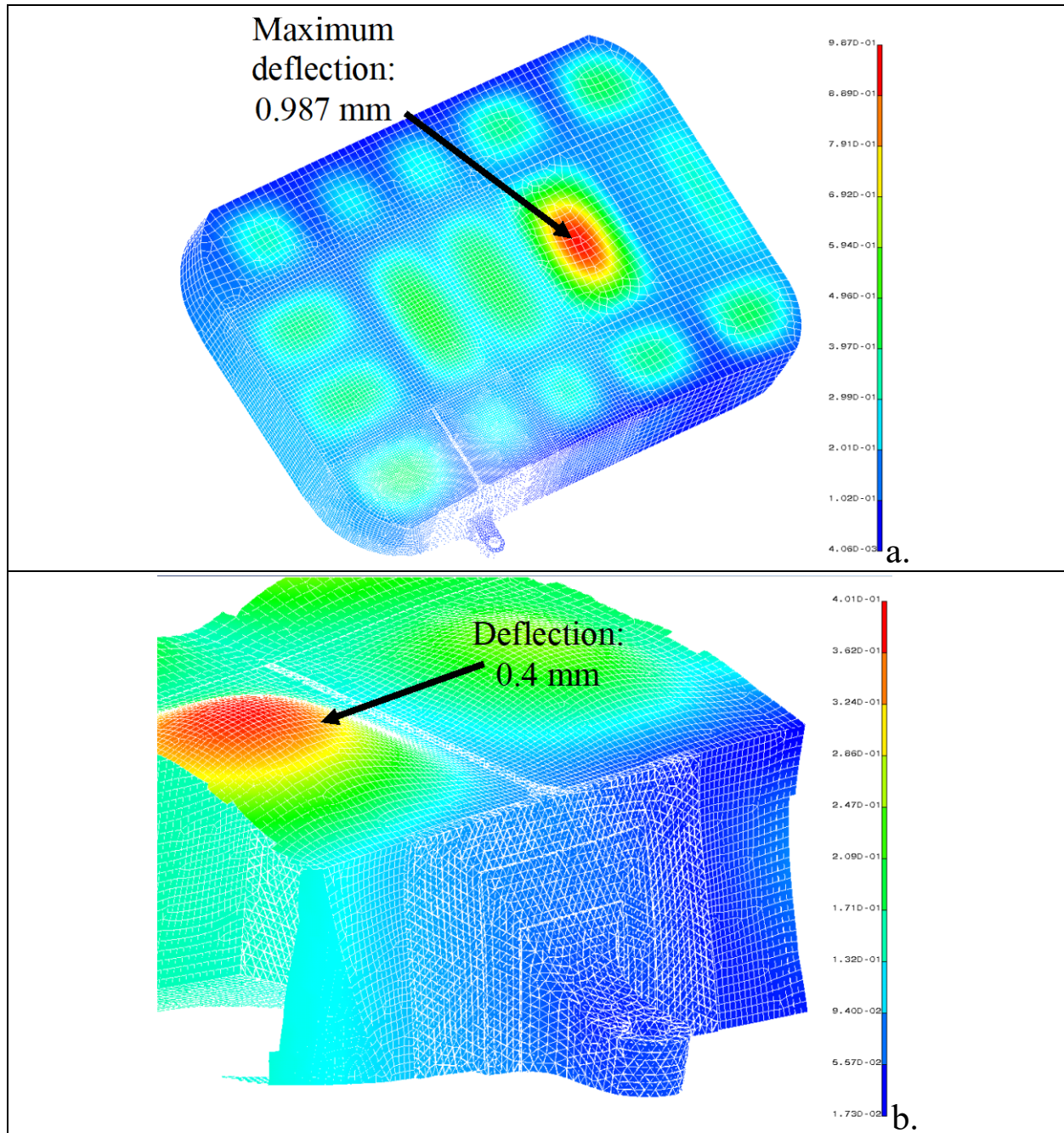


**Figure 17. Displacement results in the casting**

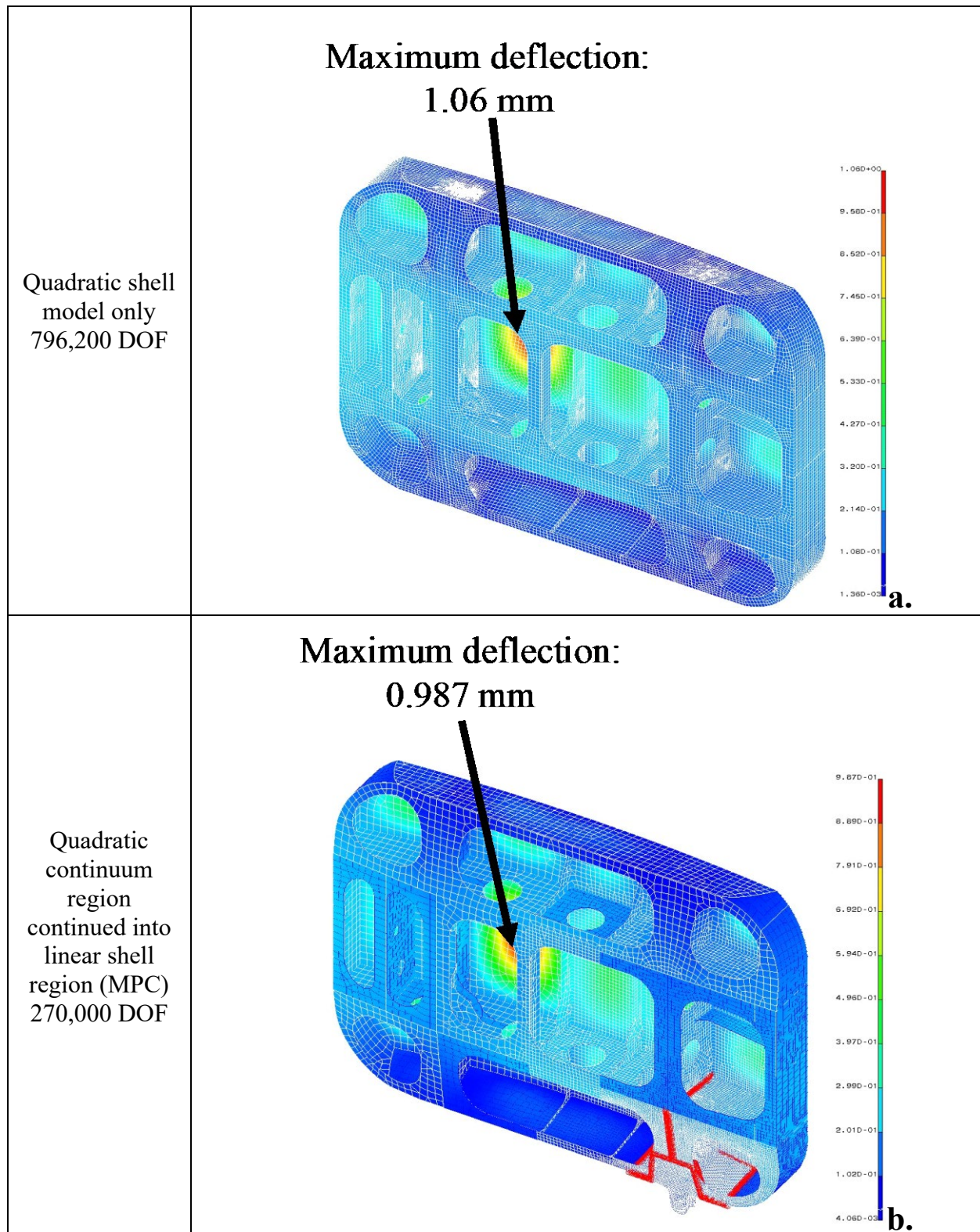


Note the displacement continuity across the shell/continuum. This continuity is shown in figure 18, showing the deformed shape of the Boeing 757 EE access door in which displacements are amplified by a factor of 500.



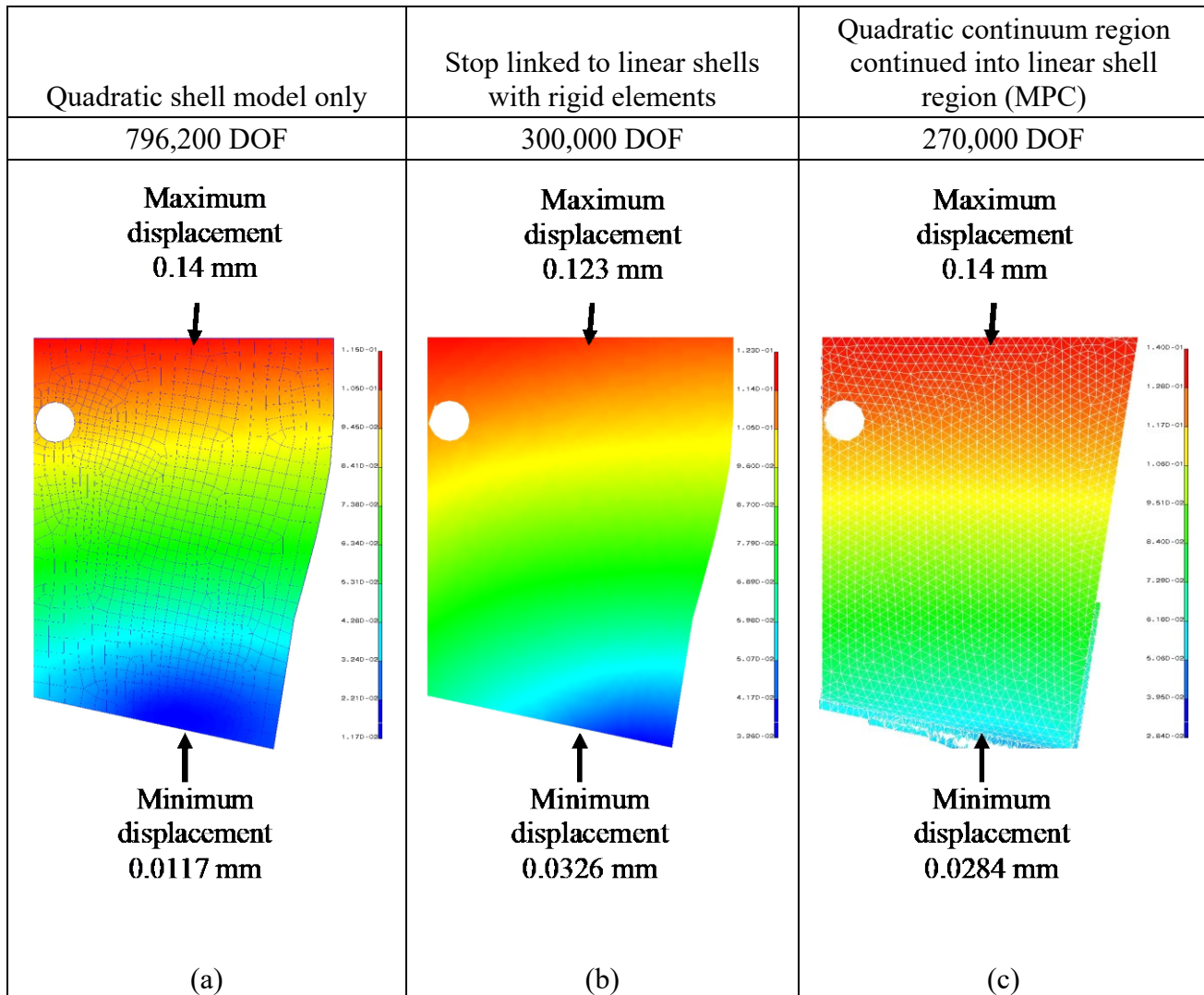
**Figure 18. Deformed shape of the casting in the stop region (amplification factor of 500)**

Figure 19 compares the displacement values obtained in this analysis to those obtained in previous analyses. Note that the displacement results are more accurate than the stress results previously shown. This stems from the fact that using a displacement-based variational principle yields a set of linear algebraic equations for the displacement values at the nodes. Strains and stresses are then approximately computed from these displacements, with additional error.



**Figure 19. Comparison of displacement values in the Boeing 757 EE access door casting for two models**

Figure 20 shows the magnitude of the displacement in the strut at the interface with the stop. Note the similar qualitative and quantitative behavior in the three models in figure 20. The current model, figure 20(c), shows comparable results with the reference solution in figure 20(a). In the model associated with figure 20(c), the fillet region and the whole stop region was modeled explicitly, whereas figure 20(a) shows the strut at the interface where the stop was modeled with an assumed constant thickness. Note that the displacements at the top of the figures (far from the filleted region) are almost identical (0.14 mm in both cases). Also, note that the presence of the stop does not significantly influence the behavior in the remainder of the component. This is a manifestation of Saint-Venant's principle for elastic and isotropic solids. This principle states that the effect of self-equilibrated loads on an object is purely local, and that stress due to such loads decays rapidly with distance.



**Figure 20. Displacement results in the stop region of the Boeing 757 EE access door casting for three models**



#### 4.1.6.3 Deformation Results

The static strength assessment of an aerospace casting also requires a deformation analysis. Figure 21 shows the deformation values in the Boeing 757 EE access door casting for the limit load  $p_l = 9 \text{ psi} = (62,053 \text{ Pa})$ . The maximum computed von Mises effective strain in the component is 0.2%.

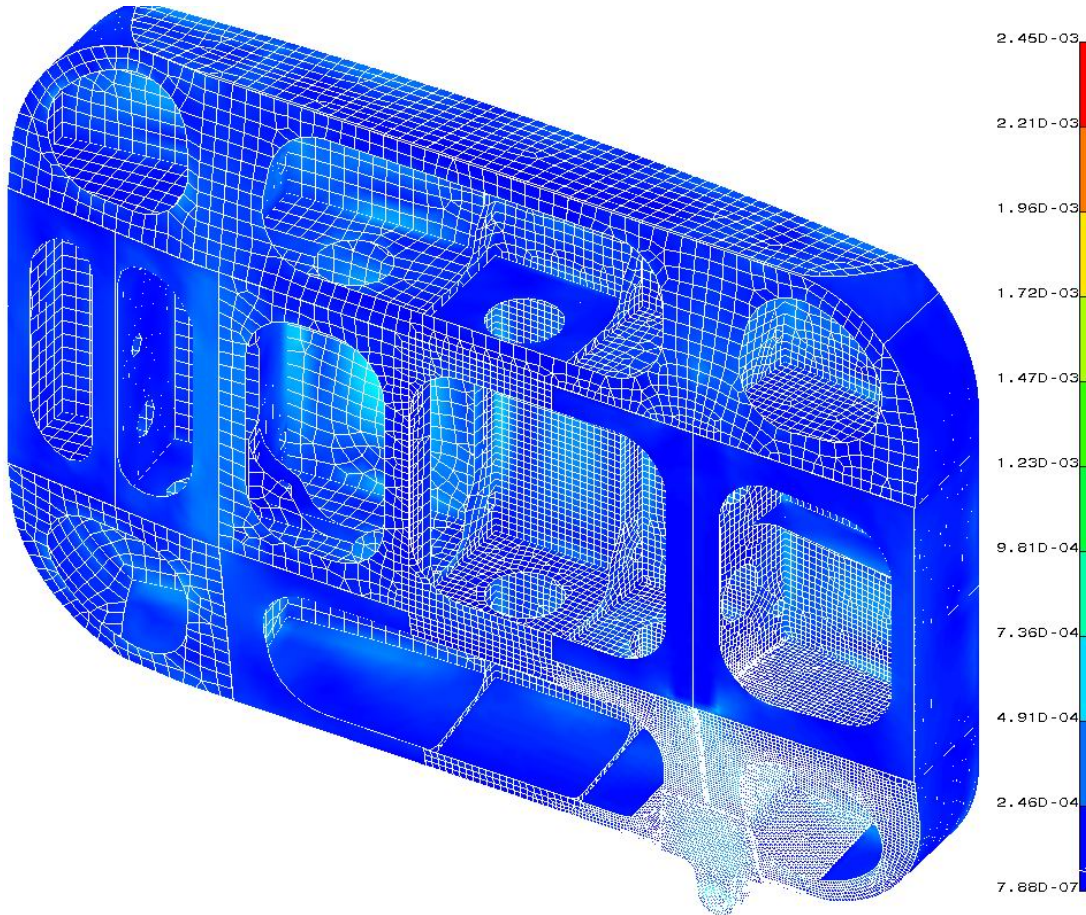


**Figure 21. Deformation in the Boeing 757 EE access door casting**

#### 4.1.6.4 Error Norm Results in the Stop Region

To assess the accuracy of the stress results presented, it is important to look at the error norm defined in reference 15. Figure 22 shows the error norm values in the strut of the stop region for the three models shown in the two previous sections.

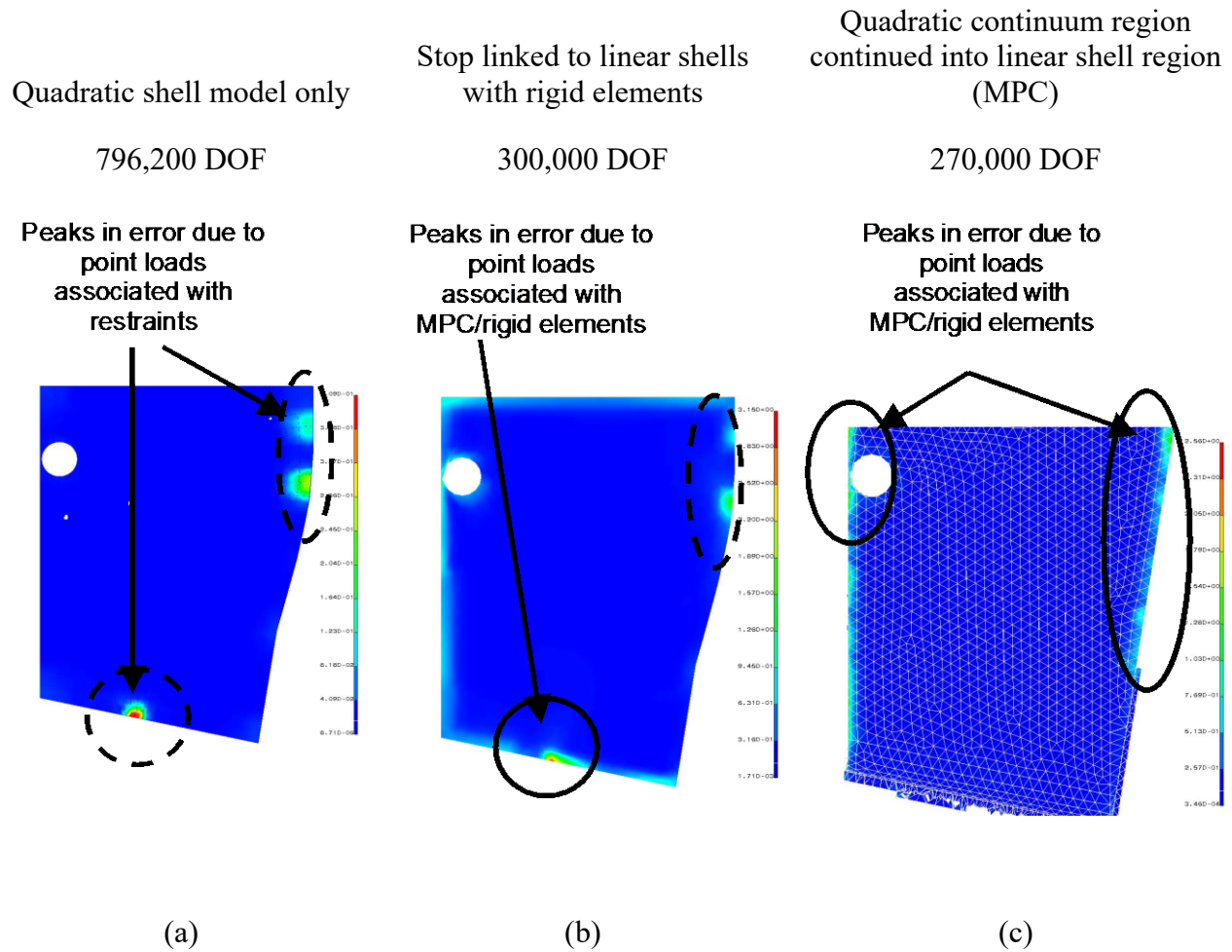


**Figure 22. Norm of error in the stress in the strut of the stop region for three models of the Boeing 757 EE access door casting**

In figures 22(a) and 22(b), spikes in the error (Zienkiewicz and Zhu's error indicator) are clearly visible at the link between the stop and the door (bottom). In figure 22(a), the spikes are due to the application of restraints in the  $z$  direction used to simulate the presence of the stop. In figure 22(b), spikes also appear and are due to the influence of the MPC elements used to link the stop to the shell-modeled structure of the door. Such spikes are not visible in figure 22(c), which shows the final modeling strategy used to assess the static strength of the door. In the latter case, spikes associated with point loads due to restraints or MPC elements are not present in the filleted region of the strut. In this region, stress values of high accuracy are desired. This behavior is noted because the interface between shell and continuum elements was moved from the region of interest to where stress values are known with a high confidence level from other models. This is shown in figure 23, where it is clearly visible that the error is higher at the interface between the continuum and the shell regions and highest at corner points.

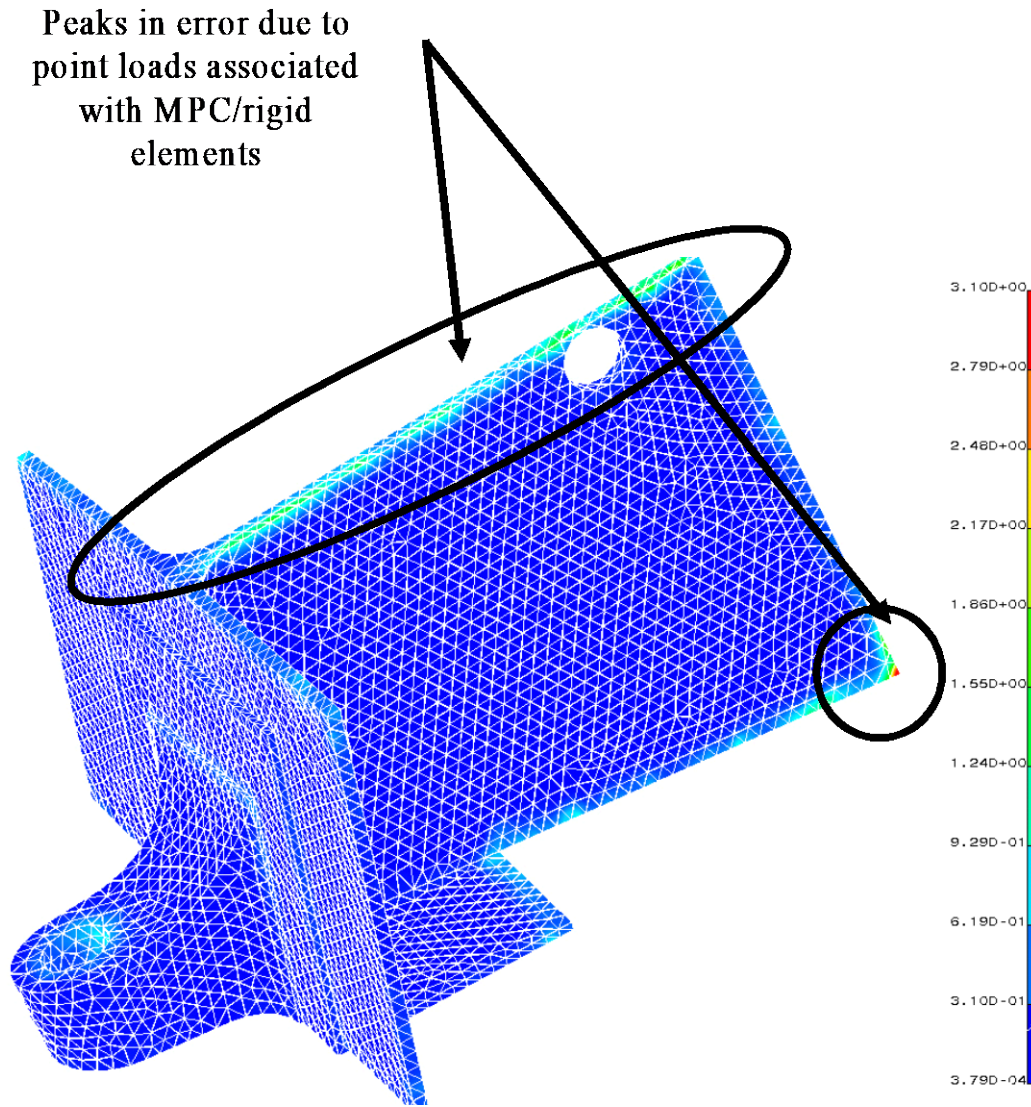


**Figure 23. Norm of error in the continuum elements representing the stop region of the Boeing 757 EE access door casting**

Section 3.1.6.5 shows that the stress field far away from the stop region remained unaffected by its more realistic modeling that supports the results presented in this section.

#### 4.1.6.5 Results Far From the Stop Region

The modification of the modeling techniques of one area in the component should not significantly influence the results in remote areas of the casting, as will be discussed in this section. Figure 24 shows the von Mises stress values for a well-refined quadratic shell model of the whole door with and approximate account of the stop restraint. It also shows values for the current model of the whole stop region, including the strut fully meshed with continuum elements.



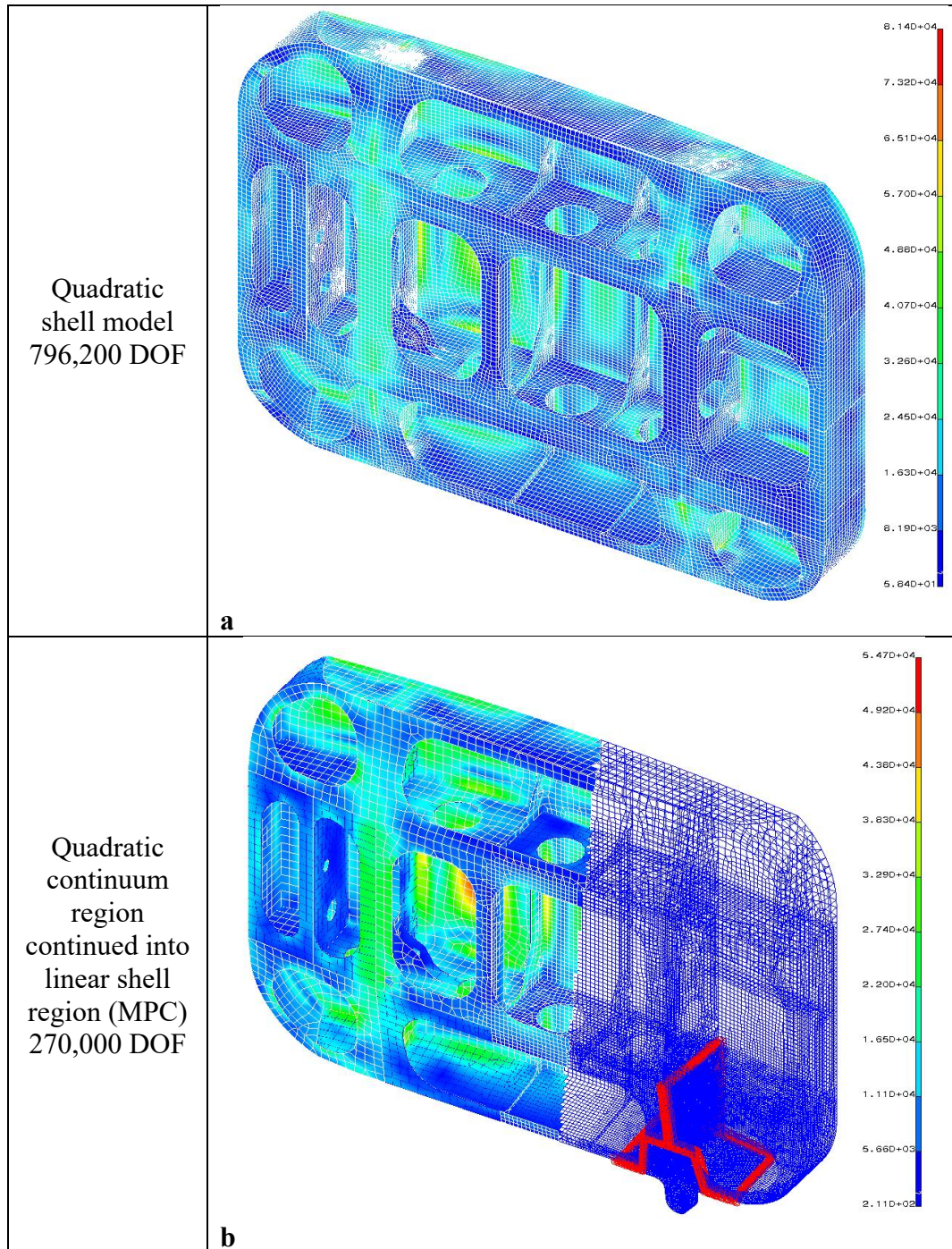


**Figure 24. Comparison of the von Mises stress values far from the stop region for two models**

It is evident from figure 24 that values of the remote stress from the stop region are unaffected by the enhanced modeling of the region. For example, the value of the von Mises stress at the center of the handle is approximately 50 MPa in both cases. This is another manifestation of Saint-Venant's principle.

#### 4.1.6.6 Conclusions

In light of the results in sections 3.1.6.5-6, the assessment of the von Mises stress values of the Boeing 757 EE access door under the limit load  $p_l = 9 \text{ psi} = (62,053 \text{ Pa})$  are:

1. The maximum stress value occurs in the stop and is 80 MPa (= 11.6 ksi).
2. In the filleted area of the transverse struts where the stops are attached, the stress values are approximately 40 MPa (= 5.8 ksi).
3. Near the handle region, at the intersection between the struts and the outside surface of the door, stress values are 50 MPa (= 7.2 ksi).
4. Away from critical regions, such as corners, boundary application regions, or material interfaces (handle location), the stress values are approximately 10 MPa (= 1.45 ksi).
5. The maximum von Mises strain value in the whole casting was estimated to be 0.2%.

The values stated here will be used in the next section to assess the static strength of the Boeing 757 EE access door casting.

#### 4.1.7 Static Strength Assessment of the Casting

##### 4.1.7.1 Casting Factors

In this section, the notion of CF as a design requirement for aerospace castings is briefly described before a few remarks are made on its use in the safe design of critical aerospace structures.

There has been tremendous progress recently in alloy chemistry control and casting processes. However, the use of castings in airframes has remained limited and most often restricted to secondary, modulus-critical structures. This limitation in the use of castings for primary, load-critical aerospace structures is mainly because of the high scatter in mechanical properties of cast components. Because of uncertainty in material properties, CFs are imposed to reduce design strength.

A CF is a requirement that reduces the tensile strength used for designing cast components made of casting alloy. The values of CF are imposed by FAA regulation 14 CFR 25.621 or specified in documents such as MMPDS. For example, if the value of the CF to be used is +0.50, or 1.50 in FAA terminology, and the minimum acceptable tensile strength (e.g., static design allowable given by MMPDS) is 300 MPa, then the design allowable tensile strength to be used would be  $300 \text{ MPa}/1.50 = 200 \text{ MPa}$ .

For instances in which sufficient test data are available, the manufacturer, on request, may be granted a CF of 1.0 by the FAA. Several military structural applications, for which no FAA approval is required, have been designed with a CF of unity [25]. A thorough examination and testing of casting aluminum alloys, such as the D357-T6 (see reference [9]), made casting-factor-free design possible in specifically controlled situations.

Note that the use of castings in the aerospace industry offers potential cost and weight savings in comparison with built-up structures [16]. Reduced machinery and assembly costs account for reductions of more than 30% in total costs. The lap joint and fasteners may be eliminated and can contribute to substantial weight reductions. The use of casting also decreases the number of fastener holes and, therefore, the number of potential crack-initiation sites. Castings, as opposed to built-up components, also allow very complex geometries to be made/manufactured. Industry efforts, both in Europe and the U.S., are striving to reduce or eliminate CFs and, therefore, make castings competitive and more widely used in fatigue-critical aircraft structures. Unfortunately, the inability to detect flaws and defects in thick sections and the lack of material data and design allowables accounting for the uncertainties inherent to castings have given them a bad reputation. Although, aerospace structures with no CFs were successfully designed and flown, and extensive material testing was conducted, CFs are still used. Table 1 shows casting factors from design and specification of aluminum airframe structural castings.

The concept of a casting exploiting the technical possibilities of new foundry processes requires close collaboration between the client and the foundry. This leads to better component optimization and is very helpful to both partners. This kind of practice has in addition always led to higher quality castings.

**Table 1. Casting factor quick guide—from design and specification of aluminum airframe structural castings (Cercast Group, A Howmet Company)**

Application	Critical Castings Class 1		Noncritical Castings					
			Class 2		Class 3		Class 4	
Zones	Critical	Noncritical	All		All		All	
No. castings to inspect	All	All	See below		See below		See below	
Inspections	Zones	Zones	Casting	Zones	Casting	Zones	Casting	Zones
Visual	100%	100%	All	100%	All	100%	All	100%
Penetrant	100%	100%	All	100%	All	100%	Table 1 MIL-2175	100%
Radiography	100%	100%	All	100%	Table 1 MIL-2175	100%	Not required	Not required
Casting Factors	CF>=1.5		1.5<CF<=2.0		1.5<CF<=2.0		CF>2.0	
Alternate Factors	1.5>CF>1.25		1.25<=CF<=1.5		1.5<CF<=2.0		1<CF<=2	
	Test		No		No other requirement		No other requirement	
	three castings for design		other		CF=1.0 w/ specification to guarantee mech. Prop.			
	ult + limit load		requirement		periodic cut-up and tests, static test 3 castings, meet loads			

#### 4.1.7.2 Material Properties, Static Design Allowables.

The aluminum casting alloy D357-T6 is subject to statistically based A- and B-basis static allowables and recorded in the federal design manual MMPDS. “A” allowables represent the strength value that is expected to be equaled or exceeded by 99% of the population with a confidence of 95%. “B” allowables represent the strength value that is expected to be equaled or exceeded by 90% of the population with a confidence of 95%. “S” allowables are also sometimes used, but they do not represent any statistical assurance and are usually the minimum values given by the governing industry specifications.

It is worth noting that if accurate statistical allowables were developed for every aerospace casting alloy, the use of CF would then be unnecessary.

In the following paragraph, the minimum specification values for D357-T6 sand composite castings [7 and 9] are reviewed. Tests were conducted by Wright Laboratory [9] on D357-T6 plates to determine the average tensile properties. The results are shown in table 2.

**Table 2. Tensile properties of the 1.25-inch-thick, water- and glycol-quenched D357-T6 plates [9]**

Foundry	Quench Medium	UTS (ksi)		YS (ksi)		El (%)	
		Avg.	Range	Avg.	Range	Avg.	Range
A	Water	54	51–55	45	44–47	5.9	3.5–8.5
	Glycol	53	51–55	43	42–44	6.6	5.5–9.0
B	Water	52	50–53	45	44–46	4.5	3.0–5.6
	Glycol	49	48–50	42	41–43	3.4	2.5–4.3
B	Water	54	53–55	47	46–48	5.4	3.9–8.2
	Glycol	51	50–52	44	43–44	4.9	4.6–5.2
Avg.	Water	53		46		5.2	
	Glycol	51		43		5	
Target Min.		50		40		3	

The minimum specification values—Ultimate Strength (UTS), Yield Strength (YS), and Elongation (El)—for D357-T6 sand composite castings for designated and non-designated areas are shown in table 2. The target values (bold in table 2) are used in this report to assess the static strength of the Boeing 757 EE access door.

Note that, as specified by 14 CFR 25.603, the suitability and durability of materials used for parts, failure of which could adversely affect safety, must:

- Be established on the basis of experience or tests.
- Conform to approved specifications (such as industry or military specifications, or Technical Standard Orders) that ensure their having the strength and other properties assumed in the design data.
- Take into account the effects of environmental conditions expected in service, such as temperature and humidity.

In the following, it is assumed that the material properties shown in table 2 conform to the three requirements above. In addition to these requirements, 14 CFR 25.613 specifies that:

- Material strength properties must be based on enough tests of material meeting approved specifications to establish design values on a statistical basis.

- Design values must be chosen to minimize the probability of structural failures due to material variability. Except as provided in paragraphs (e) and (f) of 14 CFR 25.613, compliance with this paragraph must be shown by selecting design values that ensure material strength with the following probability:
  - Applied loads are eventually distributed through a single member within an assembly, the failure of which would result in loss of structural integrity of the component, 99% probability with 95% confidence.

This means that a critical component, such as the Boeing 757 EE access door, should be designed using A or S (allowables), as defined above. In this work, A allowables are used for the material properties of the D357-T6 aluminum alloy in the static strength analysis.

- The effects of temperature on allowable stresses used for design in an essential component or structure, in which thermal effects are significant under normal operating conditions, must be considered.

As previously mentioned, the effects of temperature are considered negligible on allowable stresses, and neither account for temperature gradients nor for variation of material properties with temperature.

- Greater design values may be used if a “premium selection” of the material is made. A specimen of each individual item is tested before use to determine that the actual strength properties of that particular item will equal or exceed those used in design.

Even though the D357-T6 aluminum alloy was subjected to a myriad of tests and verifications, premium material property values will not be used for analysis so that it remains conservative.

#### 4.1.7.3 Federal Aviation Regulations

Airworthiness standards are governed by 14 CFR [1]. Chapters I and II of this publication are typically referred to as the FARs. 14 CFR Part 25 specifically covers airworthiness standards for transport category airplanes. The values of CFs that should be used for general, critical, and noncritical castings are defined in 14 CFR 25.621.

Before getting into the details of the static strength assessment of the Boeing 757 EE access door, the key terms “limit load” and “ultimate load” must be defined. The limit load is the maximum load the structure is expected to see in its lifetime or the maximum point design load condition, whichever is greater. The ultimate load is obtained by multiplying the limit load by a factor of uncertainty (formerly factor of safety) and accounting for variations in manufacture, defects not accounted for in the analysis but present in the structure, design load exceedances, and other uncertainties related to design, manufacture, and operation. Usually, this uncertainty factor is taken to be 1.5 for manned vehicles.

In the case of the Boeing 757 EE access door, the loading conditions are given by the pressure difference between its outer surface and its inner surface due to cabin pressurization. It was assumed that the limit load was 8.6 psi plus 0.4 psi for dynamic effects, resulting in an ultimate load of 13.5 psi.

The Boeing 757 EE access door is assumed to be a critical casting, which is equivalent to assuming that its failure would preclude continued safe flight and landing of the airplane or result in serious injury to occupants. As such, the 14 CFR 25.621 mandates that the following requirements be met by this cast component.

- It should have a CF of at least 1.25.
  - It should receive 100% inspection by visual, radiographic, magnetic particle, or penetrant inspection methods, or approved equivalent nondestructive inspection methods.
  -
- If its CF is less than 1.50, then three sample castings must be static tested and shown to meet
  - Strength requirements of 14 CFR 25.305 at an ultimate load corresponding to a casting factor of 1.25
  - Deformation requirements of 14 CFR 25.305 at a load of 1.15 times the limit load.

The 14 CFR 25.305 strength and deformation requirements are stated as follows:

- The structure must be able to support limit loads without detrimental permanent deformation. The deformation of the structure at the limit load may not interfere with safe operation.
- The structure must be able to support ultimate loads without failure for at least 3 seconds unless proof of strength is shown by dynamic tests simulating actual load conditions.
- Static tests conducted to the ultimate load must include the ultimate deflections and ultimate deformation induced by the loading.
- If analytical methods are used to show compliance with the ultimate load strength requirements, it must be shown that:
  - The effects of deformation are not significant.
  - The deformation involved is fully accounted for in the analysis.
  - The methods and assumptions used are sufficient to cover the effects of this deformation.
  - If the flexibility of the structure is such that transient stresses created by any rate of load application likely to occur in the operating conditions are appreciably higher than the stresses corresponding to static loads, the effect of this rate of application must be considered.
- The airplane must be designed to withstand any vibration and buffeting that might occur in any likely operating condition up to design dive speed (VD)/MD, including stall and probable inadvertent excursions beyond the boundaries of the buffet onset envelope. This must be shown by analysis, flight tests, or other tests found necessary by the administrator.

- Unless shown to be extremely improbable, the airplane must be designed to withstand any forced structural vibration resulting from any failure, malfunction, or adverse condition in the flight control system. These must be considered limit loads and must be investigated at airspeeds up to design cruising speed (VC)/MC.

#### 4.1.7.4 Design Scenarios and Assumptions

To assess the static strength of the Boeing 757 EE access door, the aforementioned requirements were reviewed using different scenarios that were examined successively.

To start, it is assumed that the inspection requirements are met. This means that the Boeing 757 EE access door castings have received visual, radiographic, magnetic particle or penetrant inspection, or have undergone an equivalent nondestructive inspection.

14 CFR 25.305 specifies that if analytical methods are used to show compliance with the ultimate load requirements, the following must be shown:

- The effects of deformation are not significant. In assessing strength and deformation requirements, the maximum computed deformation will be stated, and it will be shown that it is not significant.
- The deformation involved is fully accounted for in the analysis. This assumption will always be verified because our finite element models always fully account for deformations, assuming that the material remains in its linear elastic range.
- The methods and assumptions used in the analyses are sufficient to cover the effects of the deformation.

The present analysis is concerned with stresses induced by pressurization of the fuselage, deemed to occur at a slow enough rate so that rate or transient effects may be neglected.

In the coming analysis, the effects of vibration and buffeting that might occur in operating conditions, including stall and probable inadvertent excursions, beyond the boundaries of the buffet onset envelope are neglected. More information would be needed to make a clear and accurate assessment of these factors.

The aircraft must be designed to withstand any forced structural vibration resulting from any failure, malfunction, or adverse condition in the flight control systems. Dynamic analyses of the casting were not conducted here and the analysis will not account for such forced vibrations.

A critical component, such as the Boeing 757 EE access door, should be designed using A or S allowables, as defined in section 3.1.7.2. The static strength analysis of A allowables, shown in bold in table 2 for the material properties of the D357-T6 aluminum alloy, was used.

The effects of temperature on allowable stresses will be considered negligible and will neither account for temperature gradients nor for variation of material properties with temperature.

In the following, stress means the value of the von Mises stress measure.

Two possible scenarios are examined, depending on the chosen CF for the component:

- The Boeing 757 EE access door has a CF of more than 1.25 but less than 1.5.
- The Boeing 757 EE access door has a CF of more than 1.5.

#### 4.1.7.5 Design Scenario With a CF Between 1.25 and 1.5

In the first scenario, with the CF lower than 1.5, according to 14 CFR 25.621, three sample castings must be static tested. The casting must meet the strength requirements at an ultimate load corresponding to a CF of 1.25 and the deformation requirements of 14 CFR 25.305 at a load of 1.5 times the limit load.

The strength requirements for an ultimate load corresponding to a CF of 1.25 are checked. The limit load is 1.15 times the usual limit load to assess strength and deformation requirements:

$$p_l = 9 \text{ psi} \times 1.15 = 10.35 \text{ psi} = (73,361 \text{ Pa})$$

The ultimate load used for the analysis is 1.25 times the usual ultimate load (CF = 1.25):

$$p_u = 9 \text{ psi} \times 1.5 \times \text{CF} = 9 \text{ psi} \times 1.5 \times 1.25 = 13.5 \text{ psi} \times 1.25 = 16.875 \text{ psi} (116,349 \text{ Pa}).$$

The allowable tensile yield and ultimate strength have to account for the CF of 1.5; therefore:

$$YS = 40 \text{ ksi} / 1.5 = 26.67 \text{ ksi} = (184 \text{ MPa})$$

$$UTS = 50 \text{ ksi} / 1.5 = 33.33 \text{ ksi} (230 \text{ MPa})$$

Moreover, the elongation at break (maximum strain) is taken to be (see table 2):

$$El = 3\% (0.03)$$

Because the material is assumed linear elastic, the stress analyses described above show that for a load equal to the limit load ( $p_l = 10.35 \text{ psi} (71,361 \text{ Pa})$ ), the maximum stress in the casting is  $80 \text{ MPa} \times 1.15 (92 \text{ MPa})$ , which is less than the allowable tensile yield strength of the D357-T6 alloy ( $YS = 184 \text{ MPa}$ ). This proves that the Boeing 757 EE access door casting can sustain limit loads without detrimental permanent deformation.

Still assuming linear elastic behavior of the material, for a load equal to the ultimate load ( $p_u = 16.875 \text{ psi} (116,349 \text{ Pa})$ ), stress analyses show the maximum stress in the casting to be  $80 \text{ MPa} \times 1.5 \times 1.25 = 150 \text{ MPa}$ , a value less than the allowable tensile strength of the D357-T6 alloy ( $UTS (230 \text{ MPa})$ ). This verifies that the structure is able to support the ultimate load without failure.

Now that the strength requirements specified by 14 CFR 25.305 have been checked, the deformation requirements stated in these regulations will be examined. The adequate load for



deformation analyses is the limit load. Because the CF is less than 1.5, the usual limit load is multiplied by 1.15. Therefore, the limit load to be used for calculations is:

$$p_l = 10.35 \text{ psi} (71,361 \text{ Pa})$$

The stress analyses developed above show that the maximum deformation in the casting is:

$$\varepsilon_{\max} = 2.3 \cdot 10^{-3} = 0.23\% < 3\% = E_{\max}$$

This verifies that the maximum deformation of the structure at the limit load does not interfere with safe operation.

Note that because analytical methods were used to show compliance with the ultimate load strength requirements, the effects of deformation are not significant, which is clearly the case here.

Therefore, the Boeing 757 EE access door satisfies the deformation requirements of 14 CFR 25.305 under a limit load of 1.15 times the usual limit load of  $p_l = 9 \text{ psi} (62,053 \text{ Pa})$ .

Under the additional assumptions stated in section 3.1.7.4, this indicates that the Boeing 757 EE access door successfully passes under static strength requirements dictated by 14 CFR 25.

#### 4.1.7.6 Design Scenario with a CF of More than 1.5

If the material properties are subject to a CF of more than 1.5, then no alternate factor or extra requirements need to be imposed for the casting component to qualify under 14 CFR 25. The most conservative CF of 2.0 is used for calculations.

The limit and ultimate loads are:

$$p_l = 9 \text{ psi} (62,053 \text{ Pa})$$

$$p_u = 9 \text{ psi} \times 1.5 = 13.5 \text{ psi} (93,079 \text{ Pa})$$

The allowable tensile yield and ultimate strength have to account for the casting factor of 2.0; therefore:

$$YS = 40 \text{ ksi} / 2.0 = 20 \text{ ksi} (138 \text{ MPa})$$

$$UTS = 50 \text{ ksi} / 2.0 = 25 \text{ ksi} (172.5 \text{ MPa})$$

Under limit and ultimate loads, the associated stresses and deformations in the casting are as follows:

$$\sigma_{\max} = 80 \text{ MPa} \quad \varepsilon_{\max} = 0.2\% \quad \delta_{\max} = 1.06 \text{ mm} \quad \text{under the limit load}$$

$$\sigma_{\max} = 120 \text{ MPa} \quad \varepsilon_{\max} = 0.3\% \quad \delta_{\max} = 1.59 \text{ mm} \quad \text{under the ultimate load}$$

Consequently, the maximum stress in the Boeing 757 EE access door is less than the allowable tensile yield strength for the D357-T6 aluminum alloy, which verifies that the structure is able to support limit loads without detrimental permanent deformation.

Also, the deformation of the structure at the limit load is so small that it will certainly not interfere with safe operation of the aircraft. In particular, at the gasket location, where deformations would potentially have harmful effects on the operation of the structure, strains are the lowest with a maximum of 0.02%.

At ultimate loads, the maximum stress is well below the maximum allowable tensile strength of the aluminum alloy D357-T6, which verifies that the structure can sustain ultimate loads without failure.

Because analytical methods were used to show compliance with the ultimate load strength requirements, it must be checked that the effects of deformation have little influence on the proper functioning of the component. With deformation of approximately 0.02%, it is clearly the case here.

Therefore, the Boeing 757 EE access door satisfies the deformation requirements of 14 CFR 25.305 under a limit load of  $p_l = 9 \text{ psi}$  ( $= 62,053 \text{ Pa}$ ) and the strength requirements under an ultimate load of  $p_u = 9 \text{ psi} \times 1.5 = 13.5 \text{ psi} = 93,079 \text{ Pa}$ .

Under the additional assumptions stated in section 3.1.7.4, this suffices to assert that the Boeing 757 EE access door successfully qualifies the static strength requirements outlined in 14 CFR 25.

## 5. CONCLUDING REMARKS

The static strength assessment indicated that the Boeing 757 EE access door was designed so it passes the tests to qualify it as an aerospace component in transport category aircraft under Title 14 Code of Federal Regulations (CFR) Part 25. The maximum values used for the stress, strain, and displacement were local values. This means that stress values in noncritical areas of the casting may be much smaller than the values used to assess the static strength of the component. This implies that it may be possible to reduce the weight of this casting and still have it pass the strength and deformation requirements outlined in 14 CFR 25.

The use of numerical methods, backed up with experimental data, for stress analysis of complex aerospace components can make this optimization process feasible. If a geometrically parameterized model of the component at hand is available, modern finite element packages often allow for the assessment of the sensitivity of selected fields of interest because of the variation of selected geometrical or material parameters. For example, in the case of the Boeing 757 EE access door, sensitivity analyses can be carried out to assess the influence of the variation of the shell thickness at various locations in the component. Also, it would be interesting to see the effect of changing material properties in the handle region. Fillet radii and wall thicknesses could be used

as parameters to optimize stress values in the component. Several scenarios pertaining to boundary conditions and restraints could also be investigated to find the most efficient and suitable way to attach the door to the structure of the airplane.

It is possible that some of the strut geometries could be modified (i.e., thinned in some places), especially if a more pronounced fillet was present. However, it is important to keep the component manufacturable by avoiding zones in the casting that would be too thin.

The original defect size predicted by casting modeling and the probability of detection predicted by the nondestructive evaluation simulations should be taken into account in the iterative reassessment of the design of the casting.

## 6. REFERENCES

1. Title 14 Code of Federal Aviation Regulations: 1, 14 CFR 25.571 (2002).
2. Chong, D. (1993). Use of Titanium Castings Without A Casting Factor. *Transactions of the American Foundrymen's Society*, 101(93-26), 81–92, 950155.
3. McLellan, D. (1994). *Understanding Casting Factors in Aircraft Components*. Modern Casting, Schaumburg, IL: American Foundry Society Publications.
4. Harmsworth, C.L. (1987). "Damage Tolerant Design Without a Casting Factor," AFWAL Materials Laboratory, Wright-Patterson Air Force Base, Ohio, American Foundry Society publication Reference #87119.
5. Gruner, J., "Structural Aluminum Aircraft Castings with no Casting Factor," Northrop Grumman Corporation white paper, 4/22/96, Updated 01/08/97.
6. Rice, R.C., Jackson, J.L., Bakuckas, J., and Thompson, S. (2002). *Metallic Materials Properties Development Standards (MMPDS) Handbook*. Retrieved from [http://www.tech.purdue.edu/at/courses/at308/Technical\\_Links/MMPDS/OptionsMenu.pdf](http://www.tech.purdue.edu/at/courses/at308/Technical_Links/MMPDS/OptionsMenu.pdf)
7. Oswalt, K.J. (1987). *The Development and Application of High Strength Aluminum Casting Material Specifications*. Proceedings of the AFS Special Conference, Rosemont, IL.
8. McLellan, D.L. (1993). Allowables and Requirements for 356.0-T6 Standard Quality Castings. *Transactions of the American Foundrymen's Society*, 101(93-26), 81–92.
9. Northrop Corporation Aircraft Division Report. (1985). Durability and Damage Tolerance of Aluminum Castings. (ADA245237).
10. Conley, J.G., Moran, B., Gray, J. (1998). A New Paradigm for the Design of Safety Critical Castings. *Journal of Materials and Manufacturing, SAE Transactions*, 106.
11. AGARD Report. (1988). Casting Airworthiness. (Report No. 762).

12. Advisory Group For Aerospace Research and Development (AGARD). (1991). *Handbook on Advanced Castings*. Neuilly Sur Seine, France: AGARD.
13. Bathe, K.J. and Dvorkin, E.N. (1985). A Four-Node Plate Bending Element Based on Mindlin/Reissner Plate Theory and a Mixed Interpolation *International Journal for Numerical Methods in Engineering*, 21(2), 367–383.
14. Bathe, K.J. and Dvorkin, E.N. (1986). A Formulation of General Shell Elements - The Use of Mixed Interpolation of Tensorial Components. *International Journal for Numerical Methods in Engineering*, 22(3), 697–722.
15. Zienkiewicz, O.C. and Zhu, J.Z. (1987). Simple Error Estimator and Adaptive Procedure for Practical Engineering Analysis. *International Journal for Numerical Methods in Engineering*, 24(2), 337–357.
16. Barice, W.J. (1980). The Economic/Design Aspects of Titanium Castings for Aerospace Applications. Presented at the Fifth World Conference on Investment Casting, Paper 11, Florence.